Molecular impacts of dietary exposure to nanoplastics combined with arsenic in Canadian oysters (*Crassostrea virginica*) and bioaccumulation comparison with Caribbean oysters (*Isognomon alatus*)

Marc Lebordais, Juan Manuel Gutierrez-Villagomez, Julien Gigault, Magalie Baudrimont, Valerie S. Langlois

PII: S0045-6535(21)00801-8

DOI: https://doi.org/10.1016/j.chemosphere.2021.130331

Reference: CHEM 130331

To appear in: *ECSN*

Received Date: 21 January 2021

Revised Date: 12 March 2021

Accepted Date: 16 March 2021

Please cite this article as: Lebordais, M., Gutierrez-Villagomez, J.M., Gigault, J., Baudrimont, M., Langlois, V.S., Molecular impacts of dietary exposure to nanoplastics combined with arsenic in Canadian oysters (*Crassostrea virginica*) and bioaccumulation comparison with Caribbean oysters (*Isognomon alatus*), *Chemosphere*, https://doi.org/10.1016/j.chemosphere.2021.130331.

Credit Author Statement

Marc Lebordais: methodology, investigation, formal analysis, writing - original draft. **Juan Manuel G. Villagomez:** methodology, investigation, writing - review & editing. **Julien Gigault:** funding acquisition, resources, writing - review & editing. **Magalie Baudrimont:** funding acquisition, conceptualization, supervision, writing - review & editing. **Valerie S. Langlois:** funding acquisition, project administration, conceptualization, resources, supervision, writing - review & editing.

Molecular impacts of dietary exposure to nanoplastics combined with arsenic in Canadian oysters (*Crassostrea virginica*) and bioaccumulation comparison with Caribbean oysters (*Isognomon alatus*).

Marc Lebordais[1,2], Juan Manuel Gutierrez-Villagomez[2], Julien Gigault[3], Magalie Baudrimont[1] and Valerie S. Langlois[2]

[1]Université de Bordeaux, CNRS, UMR EPOC 5805, Place du Dr Peyneau, 33120 Arcachon, France

[2]Centre Eau Terre Environnement, Institut national de la recherche scientifique (INRS), 490 rue de la Couronne, G1K 9A9 Québec City, QC, Canada

[3]Université Laval, UMI Takuvik 3376, 1045 avenue de la Médecine, G1V 0A6 Québec City, QC, Canada

***Corresponding author**

Valérie Langlois, Ph. D.

Associate Professor

Canada Research Chair in Ecotoxicogenomics and Endocrine Disruption

Institut national de la recherche scientifique (INRS)

Centre Eau Terre Environnement

490, rue de la Couronne, Québec (Québec)

Canada G1K 9A9

T: +1.418.654.2547

E: valerie.langlois@inrs.ca

Graphical Abstract

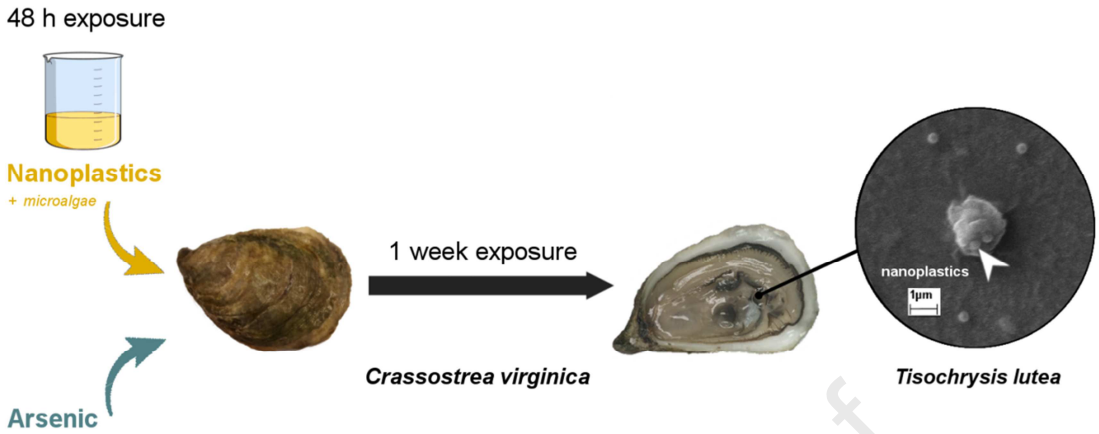

Abstract

Despite the urge need to address the possible impact of plastic debris, up to now, little is known about the translocation of nanoplastics through the trophic web. Plus, due to their surface reactivity, nanoplastics could sorb and thus increase metals bioavailability to aquatic filter-feeding organisms (e.g., bivalves). In this study we investigated the dietary exposure route on the oyster *Crassostrea virginica* through microalgae themselves exposed to three nanoplastic dispersions (PSL, PSC and NPG) at reportedly environmental concentrations combined or not with arsenic. Interactive effects of nanoplastics on arsenic bioaccumulation were studied, along with the expression of key genes in gills and visceral mass. The investigated gene functions were endocytosis (*cltc*), oxidative stress (*gapdh*, *sod3*, *cat*), mitochondrial metabolism (*12S*), cell cycle regulation (*gadd45*, *p53*), apoptosis (*bax*, *bcl-2*), detoxification (*cyp1A*, *mdr*, *mt*), and energy storage (*vit*). Results showcased that nanoplastic treatments combined with arsenic triggered synergetic effects on gene expressions. Relative mRNA level of *12S* significantly increased at 10 and 100 µg L^{-1} for NPG combined with arsenic and for PSC combined with arsenic. Relative mRNA level of *bax* increased for PSL combined with arsenic and for PSC combined with arsenic at 10 and 100 µg L^{-1} respectively. We also observed that relative arsenic bioaccumulation was significantly higher in *Crassostrea virginica* gills compared to *Isognomon alatus'*. These results are the first comparative molecular effects of nanoplastics alone and combined with arsenic investigated in farmed *C. virginica* oysters. Together with *I. alatus* results we thus shed light on species different sensitivity.

Keywords : nanoparticles, toxicity, bivalves, gene expression, bioaccumulation, Scanning Electron Microscopy

1. Introduction

Plastic contamination is of global concern (UNEP, 2001; Bank and Hasson, 2019) and approximately 10% of the annual worldwide plastic production ends up in the oceans (Mattsson *et al.*, 2019). Current estimates indicate that there are 30 million tons of plastic in the oceans, and according to projections by 2025, there will be 220 million tons (Wright and Kelly, 2017). Plastics have become ubiquitous in aquatic ecosystems to the point where they reached the Arctic polar circle (Lusher *et al.*, 2015) and the Mariana trench (Koelmans *et al.*, 2015; Chiba *et al.*, 2018). Plastic waste is persistent in the environment (Carpenter and Smith, 1972) and can last hundreds of years without being completely degraded (Barnes *et al.*, 2009; Briand 2014).

Physical abrasion, chemical, and photo-oxidations (e.g., waves, salt, UV; Gigault *et al.*, 2018a; Magrí *et al.*, 2018) can lead to plastic fragmentations resulting in the formation of microplastics (MPs) and nanoplastics (NPs). MPs are synthesized or broken plastic pieces smaller than 5 mm (Arthur *et al.*, 2009), while NPs are the colloidal fraction of the plastic debris (Lambert and Wagner, 2016; Gigault *et al.*, 2018b). Primary NPs refer to those coming from industrial synthesis and secondary NPs are those resulting from environmental degradation (Koelmans *et al.*, 2015). Both, MPs and NPs, including primary and secondary, are emerging contaminants (Richardson and Kimura, 2020) due to the limited knowledge regarding their hazardous structural properties and long-term fate in living beings. The toxicity of MPs and NPs raises concern globally since most marine species ingest plastic regularly (Gall and Thompson, 2015; Lusher *et al.*, 2017).

Recent evidences showed that organisms could excrete most of the ingested MPs; therefore, minimal translocation into the circulatory system and tissues is expected (Lusher *et al.*, 2013; Sussarellu *et al.*, 2016; Santana *et al.* 2018). However, as plastics age, they lose their physical integrity and their additives (e.g., plasticizers, UV-filters, flame-retardants, metals) and become less chemically stable (Lambert and Wagner, 2016; Wright and Kelly, 2017). Also, weathered and nanofragmentated plastics present highly reactive surface leading to adsorb numerous contaminants including metals and metalloids (Ashton *et al.*, 2010; Tien and Chen, 2013; Rochman *et al.*, 2014; Davranche *et al.*, 2019). For example, El Hadri *et al.* (2020a) revealed

that arsenic (As) was one of the most abundant metal adsorbed on plastic debris sampled on Guadeloupean beaches (a French island in the Caribbean Sea).

Despite recent improvement of NP technical analyses, data on NPs' fate and toxicity is limited (Quik *et al.*, 2011; Ter Halle *et al.*, 2017; Nguyen *et al.*, 2019). They are the least understood plastic fraction, potentially the most toxic to biologic systems by tissue bioaccumulation and vectoring chemical contamination (Nel *et al.*, 2006; Mattsson *et al.*, 2015; Chae and An, 2017). Riverine systems are the major input of plastic debris to the open ocean (Mayer and Wells, 2012; Lasareva *et al*., 2017). Therefore, since estuaries link rivers to oceans they are the key interface controlling the fate, transport and accumulation of plastics debris, more specifically for NPs (Galgani *et al.*, 2000; Browne *et al.*, 2010; Sadri and Thompson 2014). Indeed, the change in estuarine systems of ionic strength and natural organic matter (NOM) will control the aggregation of NPs. Aggregation is the main parameter affecting NPs final reactivity in regard to other contaminants. In such systems, mangroves are a specific category where these parameters are intensified (Bouillon, 2011). Moreover, mangroves are essential ecosystems weakened by anthropogenic pressure, thus they are relatively used as proxy for worldwide environmental issues (Mitra, 2013; Carugati *et al.*, 2018; Kulkarni *et al.*, 2018).

Bivalves are a class of marine and freshwater molluscs. They include oysters, clams, mussels, and most of them are filter feeders (Hancock *et al.*, 2008; Baudrimont *et al.*, 2019) also they have been used historically as biomonitoring species to assess exposure to metals (Aguirre-Rubí *et al.*, 2017; Kulkarni *et al.*, 2018). However, recently, plastic exposure to aquaculture bivalves raised concerns about NPs transfer within the food web (Baun *et al.*, 2008; Bouwmeester *et al.*, 2015; Bank and Hansson 2019). Therefore we conducted a trophic exposure using the Eastern oyster (*Crassostrea virginica)* to assess the potentially toxic effects of three distinct NPs and in combination with As. The oyster *C. virginica* is one of the most extensively farmed oyster species in the world. Due to its habitat tolerances ranging from the Gulf of Mexico to Canada's eastern bays (Ozbay *et al.*, 2014), this species is highly commercially valuable and is also commonly used in toxicity assays (McCarthy *et al.*, 2013; Ward *et al.*, 2019; Smith *et al.*, 2020). We used three NP models following a gradient of environmental relevancy : (i) carboxylated polystyrene nanoparticles of latex (PSL) free of additives as it can induce toxicity (Pikuda *et al.*,

2019), (ii) the crushed pristine polystyrene nanoparticles (PSC) that was considered more relevant in size and shape distribution, and finally (iii) nanoplastics environmentally weathered from microplastic debris collected in Guadeloupe. We analyzed *C. virginica* As bioaccumulation and gene expressions in gills and visceral mass tissues after NPs trophic exposure. Then, the As bioaccumulation factor was compared between *C. virginica* and widely caught flat tree oysters (*Isognomon alatus)* that had been previously studied (Lebordais *et al.*, *submitted*). The tropical *I. alatus* oyster is native to Caribbean mangroves that are exposed to the North Atlantic gyre where plastic debris concentrate (7^{th} expedition continent, Baudrimont *et al.*, 2019).

2. Materials and methods

2.1 Preparation of nanoplastic dispersions and size characterisation

In this study, we used three different NP dispersions : (i) spherical carboxylated polystyrene nanoparticles of latex (PSL) synthesized according to a previous protocol (Pessoni *et al*., 2019) free of additives; (ii) the crushed polystyrene nanoparticles (PSC) that were in-laboratory nanofragmented from polystyrene pristine pellets by ball-milling; (iii) and a mixture of nanoplastics produced from microplastic debris environmentally weathered and collected from a beach in Guadeloupe (NPG). The PSC and NPG plastics pellets were degraded with 99% ethanol in a blade grinder to get a primary powder and later fragmented using a planetary ball mill (El Hadri *et al.*, 2020b). The resultant powder was then dried by lyophilization to remove ethanol, then suspended in deionized water (MilliQ, Millipore, 18 MΩcm) and filtered on cellulose acetate filters (5-6 µm pore size, VWR).

To assess NP hydrodynamic diameters and population distributions, dynamic light scattering (DLS) was used. Hydrodynamic diameters of PSC and NPG dispersions were measured using non-invasive backscatter optics at 25 °C on a Zetasizer nano zs instrument (Malvern Panalytical®). The intensity fluctuations by the time were processed as a correlation function. A cumulants algorithm was used to fit this function to obtain a size distribution (z-average) and the polydispersity index (PDI). The z-averages were 692.4 ± 68.55 nm (0.441 PDI) and 1071 ± 30.65 nm (0.755 PDI) for PSC and NPG, respectively. The calibrated z-average of PSL was 390 ± 20 nm (0,002 PDI). The three NPs were suspended in deionized water. To measure NP mass concentrations in the three NP dispersions, analyses were performed by total organic carbon (TOC) on a Shimadzu® instrument with a detection limit at 0.05 $mg.L^{-1}$. Spike recovery was performed (yield = 92%) to validate the analysis accuracy.

2.2 Scanning electron microscopy observation

To observe the potential interaction between NPs and microalgae surface, we exposed the microalgae *Tisochrysis lutea* (formerly known as *Isochrysis galbana*; Bendif *et al.*, 2014) for 48 h to PSL dispersions at 0 (control), 10, 100, 1000, and

5000 µg L^{-1} and observed them using Scanning Electron Microscopy (SEM). For this, *T. lutea* was purchased from Bigelow National Center for Marine Algae and Microbiota (Maine, USA). The micro algae were aliquoted into previously cleaned glass vials (one per treatment, n = 1) and acclimatized for one week at room temperature under 24:24 artificial light. All microalgae solutions yielded the same concentration (2.1 x 10^6 cells/mL) measured on a Coulter Multisizer II particle counter (Fortin *et al.*, 2000) before starting the exposure. Right after the 48 h exposure, *T. lutea* solutions were fixed in 3% glutaraldehyde (Fisher Scientific®, United Kingdom) for 1 h (Bergami *et al.*, 2017). Samples were not previously centrifuged as we suspected PSL precipitation could cover microalgae cell walls without adsorption interactions. Micro volumes of fixed *T. lutea* were thus dried at room temperature for 30 min in a laminar hood. Later, the samples were gold sprayed and observed under SEM (Carl Zeiss EVO® 50) at 7 kV. All the glassware used in the experiments was cleaned using an acid bath of 3% nitric acid, rinsed with distilled water then with 70% ethanol and dried under a fume hood.

2.3 Microalgae and oyster cultures

Marine microalgae species *Chaetoceros calcitrans* and *Tisochrysis lutea* were obtained from Fisheries & Oceans (Tracadie-Sheila, New Brunswick, Canada). *Chaetoceros calcitrans and T. lutea* were cultured in glass balloons with F/2 medium (Guillard, 1975) at 26‰ salinity, and acclimatized at room temperature under 24:24 artificial light of 73 µmol/m²/s.

Individuals of *C. virginica* were acquired at the beginning of fall before the hibernation stage from New Brunswick's raised oysters (Canada). They were selected to have a diameter range from 6.4 to 7.6 cm, meaning all oysters were between 3 to 4 years old. Once brought to the laboratory, they were individually brushed to remove external parasites and placed in 25 L tanks (39 oysters per tank). Tanks contained reconstituted seawater (Instant Ocean®) at 30‰ salinity, oxygenated, and filtered by an aquarium filter pump. Similar to *C. virginica* farming conditions, they were acclimatized at 20 °C (Ward *et al.*, 2019) with aquarium heaters and under 12:12 (light:dark cycles) for nine weeks. During acclimation, the oysters were fed twice a week with a mixt *T. lutea* and *C. calcitrans* (2.5 x 10^6 cells/L

and 1.7 x 10^6 cells/L, per tank respectively). The algae *C. calcitrans* was used only during oysters acclimation for nutritional purposes (Gonzalez Araya *et al.*, 2012).

2.4 Trophic exposure

The microalgae *T. lutea* was used as NPs vector for *C. virginica* dietary exposition to PSL, PSC, and NPG. To that end, the three NP dispersions were separately added into *T. lutea* solutions for 48 h at nominal concentrations of 10 and 100 µg L^{-1} NPs, presumed to be environmentally low (Lenz *et al.*, 2016; Besseling *et al.*, 2014). This exposure time was chosen according to previous experiments and proven to be effective (Lebordais *et al.*, *submitted*). Before NP dosing, the microalgae concentrations were assessed by a Coulter Multisizer II particle counter (Fortin *et al.*, 2000) and brought to 4.7 x 10^6 cells/mL. NP-*T. lutea* solutions were under the same abiotic conditions as during the acclimation phase. All the *C. virginica* individuals were fed every two days with 2.24 x 10^3 cells/oyster/L of *T. lutea*. The oysters belonging to NP treatments were fed with NP-*T. lutea* at the same microalgae concentration.

To study the complexity of NP interactions with environmental metallic contaminants, we combined each NP treatment with As. Arsenate (pentoxide arsenic) is the most abundant inorganic form of As found in oxygenated marine waters and also the least toxic one (Francesconi and Edmonds, 1996; Neff, 1997; Zhang *et al.*, 2013). Therefore, a solution of dissolved arsenate (hereafter referred to As treatment) was prepared to use during the exposure (US EPA, 2001). On day one, the oysters treated with As were exposed to a nominal concentration of 1 mg L^{-1} in water (Zhang *et al.*, 2015). The As concentration was chosen based on previous studies (Langston, 1984; Zhang *et al.*, 2015) to compensate the oysters' natural chronic exposure. Water samples were collected one day out of two and the total As was measured. If needed, the As level was adjusted to keep the 1 mg L^{-1} concentration throughout the experiment.

The experimental design included twelve NP treatments, a negative control (reconstituted seawater) and a positive control (As at 1 mg L^{-1}). Thus, the experiment encompassed three single-NP treatments (NPG, PSC, PSL) at both 10 and 100 µg L^{-1} and three combined-NP treatments (also at 10 and 100 µg L^{-1} for each NPs) with

1 mg L^{-1} of As. One litre jars were filled up to 500 mL with reconstituted seawater and parafilm-covered to lower evaporative loss. Air distribution pumps were set up for water oxygenation. To avoid plastics contact, silicone tubing with glass pipette tips were used in each jar. Salinity, temperature, and light were the same as during acclimation. All treatments were conducted in five independent replicates with one oyster per glass jar. Oysters were dissected at the end of the one-week diet exposure. Biometric data are reported in supplementary file **Fig. S1**. Shell length was assessed on individual oyster pictures by ImageJ software. Whole-body were manually dried with paper then weighed (fresh weight). Gills and visceral mass tissues were quickly collected and stored at -80 °C for As dosage and subsequent molecular assays. The condition index (CI; Lucas and Beninger, 1985) was calculated by the following equation.

Equation 1 :

$$CI = \frac{\text{leftover tissues} * \text{weight}}{\text{shells weight}} \times 100 \qquad * \text{leftover tissues: whole body excluding gills and visceral mass}$$

2.5 Arsenic quantification in water by ICP-OES and in oyster tissues by ICP-MS

Total $As_{(water)}$ concentration was monitored throughout the one-week exposure. Water samples of 10 mL per jar were collected for control and As treated oysters. Then, the water samples were acidified with 3% nitric acid for inductively coupled plasma optical emission spectrometry (ICP-OES) analysis with a detection limit for As at 0.005 mg L^{-1}.

Total $As_{(tissues)}$ concentration was measured in gills and visceral mass for *C. virginica*. First dried at 50 °C for 48 h, tissues were then weighed before digestion. Tissue samples were acidified with 70% nitric acid (3 mL per sample) and heated at 100 °C for 3 h. After dilution of the digestates with deionized water (1:36), the final volume was 7 mL per sample. Concentrations of total $As_{(tissues)}$ were measured using an inductively coupled plasma mass spectrometry (ICP-MS) with a detection limit for As at 0.02 µg L^{-1}. A standard curve of an As reference solution (SCP Science®, Multi-Element Std) was systematically analyzed with the samples to control the

measured concentrations. The single spike recovery method was performed (yield = 101.71%) to validate the analysis accuracy (Wolle and Conklin, 2018).

2.6 Comparison of As bioaccumulation factor

In previous work, wild-caught *Isognomon alatus* oysters native to the Caribbean Sea were collected from Guadeloupean mangroves (Lebordais *et al.*, *submitted*). *Isognomon alatus* underwent similar acclimation and exposure conditions with *Crassostrea virginica.* These consistent parameters allow us to compare the As uptake for each oyster species. Therefore, the potential differences in the As bioaccumulation between *I. alatus* and *C. virginica* should be mainly due to their physiological and natural background differences (Moreira *et al.*, 2018). To compare As bioaccumulation levels between both oyster species, we normalized the concentration from exposed individuals to controls and presented it for gills and visceral mass.

The bioaccumulation factor (BAF) of As was calculated for *C. virginica* and *I. alatus* oysters using Equation 2 (n = 4 per treatment and species). Wet weights were calculated from the measured dry weights with 0.2 and 0.1 corrections factor for gills and visceral mass, respectively (Klinck *et al.*, 1992; Choi *et al.*, 1993; Kobayashi *et al.*, 1997). The As concentrations measured in exposed oysters were normalized with natural As background from control oysters. These relative As concentrations in gills and visceral mass were then averaged to estimate oyster's whole body content. As concentrations in water were measured for each oyster jars.

Equation 2 :

$$BAF = \frac{[As]_{\text{wet tissue}}}{[As]_{\text{water}}} \qquad \begin{matrix} [As]_{\text{wet tissue}} : \text{in } \mu g/kg \\ [As]_{\text{water}} : \text{in } \mu g/L \end{matrix}$$

2.7 RNA extraction and cDNA synthesis

A similar amount of tissues were individually homogenized with one stainless steel ball (5 mm) per sample in 600 µL of RNA lysis buffer. To that end, a Retsch® mixer mill MM 400 (Fisher Scientific®, Toronto, Canada) was used for 4 min at 20 Hz.

Oyster tissues are rich in fat and proteins and to separate these components, 500 µL of Phenol:Chloroform:Isoamyl Alcohol (25:24:1 v/v/v, Sigma-Aldrich®, Oakville, Canada) were added and vortexed before RNA extraction. This organic solvent is indeed highly suitable for insoluble tissue extractions (Vicient and Delseny, 1999). To separate the aqueous phase that contained the RNA, the samples were centrifuged for 1 min at 13,000 rpm. From there, total RNA was extracted using the Quick-RNA™ Miniprep Kit (Zymo Research®) with on-column DNAase I treatment as described in the manufacturer's protocol. The total RNA concentration was measured using a NanoDrop-2000 spectrophotometer (Thermo Fisher Scientific®). The nucleic acid purity was ensured by ratios 260/280 > 1.8 and the RNA integrity of each sample was assessed on a 1% agarose gel. Generally, in eukaryotes the RNA integrity is assessed by the presence of two defined bands representing the 28S and 18S ribosomic RNA (rRNA) (Gutierrez-Villagomez *et al.*, 2019). In the RNA integrity analysis, a single band with no smear was observed in the gels. This is possible due to a "hidden break" in the 28S rRNA of *C. virginica* after heat denaturation. Winnebeck *et al.* (2010) documented the 28S rRNA splits into two fragments that overlap with the 18S rRNA during a gel electrophoresis.

All the samples were diluted to obtain the same RNA concentration (2000 ng in 8 µL). Complementary DNA (cDNA) was prepared using Maxima™ H Minus First Strand cDNA Synthesis Kit with dsDNase (Thermo Fisher Scientific®). A first step of DNA denaturation was conducted with dsDNase according to the supplier's instructions. Then 4 µL of mix including the reverse transcriptase enzyme, buffer and primers were added with 6 µL of water per sample. This second step was performed on a Mastercycler Thermocycler Pro S (ThermoFisher, Ottawa, Canada) following the supplier's protocol. All cDNA was synthesized at the same time for each tissue sample including a no reverse transcriptase control (NRT) and a no template control (NTC). Then the cDNA samples were stored at -20 °C.

2.8 qPCR assays and validations

Quantitative polymerase chain reaction (qPCR) was performed to measure relative messenger RNA (mRNA) levels in the following 15 genes : clathrin heavy chain (cltc) to evaluate endocytosis; catalase (*cat*), glyceraldehyde-3-phosphate-deshydrogenase (*gapdh*) and superoxide dismutase Cu/Zn extracellular (*sod3*) to

assess oxidative stress; mitochondrial encoded 12S rRNA (*12S*) to measure mitochondrial metabolism; growth arrest DNA damage (*gadd45*) and tumor protein P53 (*p53*) to measure cell cycle regulation; blcl-2-associated X apoptosis regulator (*bax*) and apoptosis regulator (*bcl-2*) to assess apoptosis; cytochrome P450 family 1 sub-family A1 (*cyp1A*), ATP binding cassette sub-family B1 (*mdr*) and metallothionein (*mt*) to assess detoxification; and vitellogenin (*vit*) to evaluate the energy storage. Elongation factor 1 alpha (*ef1α*) and ribosomal protein L7 (*rpl7*) were included as reference genes (Lee and Nam, 2016). Specific primer sets were designed for all genes with primer-BLAST on the NCBI platform (supplementary file **Table S1**) and synthesized by Sigma-Aldrich®. The complete details concerning the qPCR analysis is summarized in the Supplementary materials.

2.9 Statistical analyses

Analysis of outliers for biometric data, relative mRNA levels and As tissue concentrations were performed using the ROUT method (Q = 1%) in GraphPad Prism 8.0 (Motulsky and Brown, 2006). Raw data were then transformed by commonly used functions (square root, double square root or decimal logarithm) to satisfy parametric conditions in SigmaPlot 12.0. Normality was thus confirmed using Shapiro-Wilk test and homoscedasticity was confirmed by Levene test. Transformed data were compared using a two-way analysis of variance (ANOVA) for biometric data and relative mRNA levels. As bioaccumulation transformed data were only compared using a one-way ANOVA or a Student's t-test. For all data, the significant differences were identified by a post-hoc Tukey HSD test on Prism 8.0. The significance level was set at $\alpha = 0.05$.

3. Results and Discussion

3.1 Bottom-up complexity of nanoplastic dispersions

We selected monodispersed PSL nanoparticles free of additives to exclude chemicals toxicity. Also, PSL were functionalized with carboxylated groups making them stable and optimal for comparing results with literature in regard to impact determination of NPs (Kim *et al.*, 2017; Thiagarajan *et al.*, 2019). Previous works already described these PSL (Pessoni *et al.*, 2019; Lebordais *et al.*, *submitted*), hence NPs characterization was focused on PSC and NPG. The PSC nanoparticles

were relevant NPs as they have been laboratory nanofragmented from large plastic pellets (El Hadri *et al.*, 2020b). As a result, they were polydispersed and covering the global colloidal size distribution (**Fig. 1 A-B**). This parameter is interesting since NPs polydispersity is poorly addressed in ecotoxicological studies (Alimi *et al.*, 2018; Bhagat *et al.*, 2020). Moreover, PSC had higher specific surface area and irregular shapes increasing NP adsorption ability compared to PSL (Quik *et al.*, 2011; Brennecke *et al.*, 2016). However, both PSL and PSC lacked natural aging and exposure to contaminants. To go one step further in the environmental relevancy, the collected Guadeloupean plastics have been naturally exposed to contaminants and weathered by abiotic processes (such as UV light) which increase surface oxidation (Holmes *et al.*, 2014; Andrady, 2017; Dawson *et al.*, 2018; El Hadri *et al.*, 2020b; Mao *et al.*, 2020). Therefore, NPG resulting from plastic debris was most likely to reproduce the heterogeneity of NPs observed in the environment. As such, NPG could include several plastic polymers (e.g., polyethylene, polypropylene, polyvinyl chloride and polystyrene; Gigault *et al.*, 2016; Davranche *et al.*, 2020).

The NPG plastics mixture may also contain a wide variability of additives like pigments (Frias *et al.*, 2010). Noteworthy, pigments absorbance have been previsouly documented to bias the measures of light dispersion (Zook *et al.*, 2011; Geißler *et al.*, 2015). As NPG are detected by dynamic light scattering, they present a Brownian motion in aqueous system and therefore can be defined as NPs (Gigault et *al.*, 2018b). Based on the instensity of light scattered, NPG z-average was 1071 ± 30.65 nm. However, it is well known in the colloidal field that for large size distribution the presence of bigger particles contributes significantly to the intensity of light scattered ($I_\theta \approx r^6$, r the particle radius) compared to smaller particles. Such high polydispersity tend to mask the presence and characterization of lower size distribution in the colloidal dispersions of materials using CONTIN algorithm. (**Fig. 1 C-D**). Moreover, NPG dispersions present irregular shapes, high surface oxidation and specific surface area increasing their adsorption properties (El Hadri *et al.*, 2020a). Numerous contaminant and pollutant families can thus interact with environmental NPs, but also change their bioavailability and toxicity (Alimi *et al.*, 2018; Bhagat *et al.*, 2020). Therefore adding environmentally weathered plastics brings relevance to NP ecotoxicological studies.

3.2 Adsorption of nanoplastics on microalgae

The SEM observations highlighted that PSL was adsorbed on *T. lutea* surface in all of the tested concentrations (**Fig. 2**). At environmentally realistic NP concentrations, 10 and 100 µg L^{-1}, we observed fewer adsorbed PSL per microalgae (**Fig. 2 B-C**) compared to the higher concentrated treatments (**Fig. 2 D-E**). Noteworthy, PSL aggregates consistently appeared starting at 1000 µg L^{-1} (**Fig. 2 D**). No differences were observed in the number of adsorbed PSL between 1000 and 5000 µg L^{-1}, suggesting a saturation of the particles onto microalgae surfaces. Although these results are representative of a short exposure (48 h) in estuarine-like conditions. Indeed *T. lutea* solutions were homogenized twice a day to mimic dynamic interactions and to avoid sedimentation. In general, we did not notice damage on the microalgae surface. This result is contradictory with Wang *et al.* (2020) that observed fragmented shapes and cracked surfaces onto marine microalgae exposed for 96 h to 200 and 2000 µg L^{-1} of PS NPs (70 nm) associated with molecular and physiological hazards. Such difference can be potentially explained by the presence of surfactant and additives generally used for commercially available PSL (Pikuda *et al.*, 2018). Unlike PSC and NPG, PSL were a valuable NPs model easy to target by SEM given their consistent spherical shape. Also, Pessoni *et al.* (2019) previously demonstrated the PSL carboxylated surface functions should prevent them from forming homoaggregates. Nonetheless, PSL most likely formed heteroaggregates in the presence of NOM noticeable as clear dots in the SEM observations (**Fig. 2**). NP aggregations had been observed to change their bioavailability, and thus, to either increase or decrease NP toxicity (Corsi *et al.*, 2014; Zhang *et al.*, 2018). Surprinsigly, despite PSL heteroaggregations and their global negatively charged surface, the SEM images showed that PSL was able to adsorb onto microalgae regardless of natural organic matter's presence and for all the tested concentrations.

3.3 Oysters physiology and arsenic bioaccumulation

3.3.1 Biometric parameters and arsenic uptake

Crassostrea virginica's biometric data are presented in **Fig. S1**. The registered mortality during the exposure was minor (7%) and statistical differences were only detected for fresh tissue weight (**Fig. S1 A**). Nonetheless, there were no significant

differences between the control and other treatments, between both concentrations of the same NP treatment, nor between the As treatment and the NP + As treatments (**Fig. S1 A**).

Crassostrea virginica oysters from control treatment had an average As concentration of 1.6 µg g^{-1} (dry weight) in gills and 3.5 µg g^{-1} in visceral mass (**Fig. 3**). As-exposed oysters (As and NPs + As treatments) displayed significantly different levels of total As compared to the control treatment, around 5 fold-change for both *C. virginica* tissues. In perspective with oysters' capacity to bioaccumulate As in several orders of magnitude higher (Zhang *et al.*, 2015), our 1 mg L^{-1} treatment does not suggest an excessive As exposure. Yet, all As-exposed oysters accumulated statistically similar levels of total As respectively to each tissue. Thereby, the NP treatments at 100 µg L^{-1} did not significantly influence the total As accumulation in *C. virginica* after one-week exposure. We observed similar results for *I. alatus* oysters that were exposed to NPG + As (Lebordais *et al.*, *submitted*). In both oyster experiments with comparable NP and As levels, the presence of NPs did not affect the total As bioaccumulation in any oyster tissues. It seems that NP exposures at environmentally realistic concentrations were not sufficient to change the total As bioaccumulation by adsorption. These observations could also witness the low adsorption affinity of arsenate (an oxy-anion) towards the negatively charged carboxylated functions onto the three NPs surface.

Indeed, these results are consistent with an environmental range of total accumulated As (from 4.1 to 39 µg g^{-1}, dry weight) in *C. virginica* individuals from Gulf of Mexico coastal areas (Wilson *et al.*, 1992). To better assess and compare oysters bioaccumulation, their native background should be considered. The *C. virginica* oysters were farmed at St-Simon bay that is connected to Chaleur bay, where controlled effluents from industrial activities have been discarded. The Human Health Risk Assessment survey (Ministère de la Santé et du Mieux-être du Nouveau Brunswick, 2005) has revealed a total As concentration up to 2 mg kg^{-1} (wet weight) in local mussels. This background value is consistent with our measured total As levels in *C. virginica* with an average of 0.7 mg kg^{-1} (wet weight) in gills and 1.4 mg kg^{-1} in visceral mass for control. Of note, wet weight tissues have a limited relevance to assess metals accumulation, yet we calculated *C. virginica* wet weights in order to make the previous comparisons. These bioaccumulation comparisons between in-

422 laboratory and wild bivalves can be made since metals kinetic accumulation are well-
423 known. Indeed non-essential metals (such as As for oysters, Rodney *et al.*, 2007; Ali
424 and Khan, 2019) usually bioaccumulate with high rates reaching their peak during
425 the first weeks post exposure followed by a plateau (Wallner-Kersanach *et al.*, 2000).
426 It is thus expected that our exposed *C. virginica* would quickly bioaccumulate As up
427 to comparative levels as those measured in wild *C. virginica* lifetime exposed to As.

428

429 *3.3.2 Species bioaccumulation factor comparison*

430 In a previous experiment, Caribbean flat oysters *I. alatus* from Guadeloupe
431 mangrove swamps were also exposed in-laboratory to 1 mg L^{-1} of As for one week
432 (Lebordais *et al.*, *submitted*). *I. alatus* and *C. virginica* underwent identical
433 experimental conditions regarding microalgae feeding, salinity, temperature, and
434 light conditions. The relative As bioaccumulation yielded 2-fold change in *I. alatus*
435 tissues compared to controls, while *C. virginica* yielded approximately 5- to 10-fold
436 change in gills and visceral mass, respectively (**Fig. 4**). There was a significant
437 difference between the gills of *I. alatus* and *C. virginica*. In most aquatic organisms,
438 gills are known to be a transport organ for metallic contaminants (Kraemer *et al.*,
439 2005; Won *et al.*, 2016, Cao et al; 2018). As gills respond rapidly to metal
440 contamination in water, they have a short-term role in regulation (Langston, 1984;
441 Strady *et al.*, 2011). Ultimately, they are more sensitive through waterborne
442 contamination until metals move into storage organs, like the visceral mass
443 (Soegianto *et al.*, 2013; Arini *et al.*, 2014). As expected, high As concentrations were
444 measured in *I. alatus* oysters exposed in a laboratory setting (Lebordais *et al.*,
445 *submitted*). Nonetheless, relative As levels suggested higher As uptakes for exposed
446 *C. virginica* oysters (**Fig. 4**).

447 We then calculated the BAF using wet weight for each oyster species. Whole-
448 body BAFs estimated from gills and visceral mass were 13.4 (± 6.1) for *I. alatus* and
449 57.7 (± 41.9) for *C. virginica*. These BAF values confirmed a higher As uptake for *C.*
450 *virginica* individuals compared to *I. alatus* suggesting *I. alatus'* physiology is
451 potentially adapted to grow into As-rich environments (Cherkasov *et al.*, 2010; Luo *et*
452 *al.*, 2014). Regulation, biotransformation, and/or detoxification mechanisms may
453 enable *I. alatus* to tolerate higher As concentrations as revealed by the major As

454 bioaccumulation baseline in the control treatment. Consequently, *C. virginica* is
455 presumably more vulnerable to As exposure than *I. alatus*. Indeed, New Brunswick's
456 nurseries and bays carried most likely minimal As availability to *C. virginica* (as
457 revealed by the low As bioaccumulation baseline in controls). Moreover, BAF
458 standard deviations show noticeable contrast for each species. This difference might
459 be related to oysters filtration rates. *Isognomon alatus* oysters showed consistent
460 BAF values between individuals, while *C. virginica* showed a higher BAF variability
461 between individuals. This high variability could be explained by a putative change in
462 filtration rates between *C. virginica* oysters trying to protect themselves from metal
463 contamination (Tran *et al.*, 2003; Pan and Wang, 2012; Freiras *et al.*, 2018).

464 The gills and visceral mass of exposed *I. alatus* accumulated 10 and 20 times
465 more As than *C. virginica* tissues, respectively (Lebordais *et al.*, *submitted*). However,
466 As bioaccumulation was already higher in *I. alatus* controls than in exposed *C.*
467 *virginica* oysters. This major difference could be due to the oyster's respective
468 habitats. The As concentration measured in Guadeloupean seawater was below the
469 limit of detection, and As concentration in upper St. Lawrence estuary (Quebec,
470 Canada) can be up to 1.5 µg L^{-1} for the highest salinity (Tremblay and Gobeil, 1990).
471 There is little variability of As levels in seawater, and according to Neff (1997) the
472 concentration in clean coastal and oceans ranges within 1-3 µg L^{-1}. Thus, it can be
473 considered both species were in waters with naturally similar As concentrations.
474 Nonetheless, sediment plays a key role in As waterborne route for filter-feeding
475 bivalves (Langston, 1984; Zhang *et al.*, 2013; Maher *et al.*, 2018). Consequently, As
476 concentrations in Toucari bay (close to the Guadeloupe island) ranged from 27.8 to
477 40.9 mg kg^{-1} in submarine sediment (Johnson and Cronan, 2001); whereas, the
478 average As concentration in Chaleur bay sediment (New Brunswick, Canada) was
479 11 mg kg^{-1} (Parsons and Cranston, 2005). Also, As is accumulated by primary
480 producers like phytoplankton being the main As dietary route for marine consumer
481 organisms (Neff, 1997; Azizur Rahman *et al.*, 2012; Maher *et al.*, 2018) and warmer
482 water temperatures can facilitate total As uptake for bivalves (Ünlü and Fowler, 1979;
483 Gutierrez-Galindo *et al.*, 1994). As such, tropical *I. alatus* oysters grew in mangrove
484 swamps that are productive ecosystems with major sediment and phytoplankton
485 inputs (Saed *et al.*, 2004; Bouillon, 2011; Yap *et al.*, 2011). In contrast, subarctic *C.*
486 *virginica* oysters were farmed inside floating gears in less rich waters from a

Canada's Eastern bay. The age of the oysters should also be considered as it might have influenced the As accumulation results. *C. virginica* oysters were three to four years old, while *I. alatus* oysters were about six years old based on this oyster growth rate in Jamaica mangroves (nearby Guadeloupe island, Siung, 1980). Overall, As concentrations measured in both oyster controls witnessed their natural As burden that is representative of their respective habitat.

3.4 Oysters gene responses after exposure

3.4.1 Relative gene expression in gills and visceral mass

We selected a set of genes of interest to target ecotoxicological endpoints gathered in seven biological functions, such as endocytosis (*cltc*), oxidative stress (*cat*, *gapdh*, *sod3*), mitochondrial metabolism (*12S*), cell cycle regulation (*gadd45*, *p53*), apoptosis (*bax*, *bcl-2*), detoxification (*cyp1A*, *mdr*, *mt*), and energy storage (*vit*) (**Table S1**). Of note, we did not detect *vit* in gills after PCR and agarose gel analysis; thereby we only show its results for visceral mass. The **figures 5** and **6** show the relative mRNA levels results for gills and visceral mass, respectively.

The expression of *12S* significantly increased with PSL treatment at 10 µg L^{-1} compared to the control treatment, but it did not increase at 100 µg L^{-1} (**Fig. 5 A**). The exposure to PSL + As at 10 µg L^{-1} did not affect significantly the expression of *12S,* suggesting that the induction for PSL treatment at 10 µg L^{-1} was prevented by the presence of As. Similar antagonist effects of As in mixture with PSL were observed in *I. alatus* exposure (Lebordais *et al.*, *submitted*). Ribosomic RNA (rRNA) *12S* is transcribed by the mitochondrial genome. Therefore, *12S* rRNA level is used as a proxy to represent the number of mitochondrial copies in a given tissue (Al kaddissi *et al.*, 2012; Arini *et al.*, 2015). Considering that gills are involved in respiration, their mitochondrial activity can be more sensitive to contaminants like metals (Akberali and Earnshaw, 1982). Significant differences in *12S* expression for As treatment were expected in gills through waterborne route. Instead, the data suggest that As was more available through the dietary route (**Fig. 6 C**). The expression of *bax* significantly increased in the PSC + As treatment at 100 µg L^{-1} compared to control, As alone and PSC at 100 µg L^{-1} treatments (**Fig. 5 B**). Also, the *bax* expression for PSL + As treatment significantly increased at 10 µg L^{-1}, but it did

not change significantly at 100 µg L^{-1}. In addition, PSL + As at 10 µg L^{-1} significantly increased compared to control, As alone and PSL at 10 µg L^{-1} treatments. Overall, the presence of As in PSC at 10 µg L^{-1} and PSL at 100 µg L^{-1} induced a synergetic *bax* expression. *Bcl-2* gene family are central regulators of programmed cell death. Indeed, the intrinsic pathway for apoptosis relies on upregulation of pro-apoptotic genes like *bax* (Schuler *et al.*, 2000; Chipuk *et al.*, 2010). Seen *bax* regulation integrates internal and external stress signals, its expression gives a relevant proxy to assess contaminant toxicities at the cell level (Yanan 2012). For example, Cao *et al.* (2018) observed a significant increase of *bax* relative mRNA level in *Crassostrea gigas* gills and observed apoptosis at 10 µg L^{-1} of Cd. As such, the combination of As treatment with PSC and PSL most likely induced apoptotic effects in *C. virginica* after one week of exposure. The expression of *gapdh* significantly increased in PSC + As treatment at 10 µg L^{-1} compared to control and PSC at 10 µg L^{-1} treatments (**Fig. 5 C**). The *gapdh* response can be associated to oxidative stress responses but no further interpretation can be made since its protein is involved in the nucleus, mitochondrial and cytosolic signal pathways (Sirover 2011, Tristan *et al.*, 2011).

The expression of *12S* significantly increased for NPG + As treatment at 10 and 100 µg L^{-1} compared to control, As alone and NPG at 10 and 100 µg L^{-1} treatments (**Fig. 6 C**). Similarly, the expression of *12S* significantly increased in PSC + As treatment at 10 and 100 µg L^{-1} compared to control, to As alone, and PSC (at both concentrations). Thus the presence of As in NPG + As and PSC + As induced a synergetic *12S* expression. Also, PSL + As treatment significantly increased *12S* expression at 100 µg L^{-1} compared to control, As alone and PSL + As at 10 µg L^{-1} treatments. Based on these gene expression profiles, As treatment alone did not affect mitochondrial metabolism. Yet, in the presence of NPs the results could suggest that As was more effective in impairing mitochondrial metabolism like respiration. Indeed, metal toxicity can decrease oxygen consumption in mitochondria (Sokolova *et al.*, 2005; Cherkasov *et al.*, 2010). We expected mitochondrial gene response to be less sensitive to As exposure in visceral mass (Akberali and Earnshaw, 1982). Nonetheless, the mRNA level of *12S* for NPs + As treatments was significantly higher only in visceral mass. These results support stronger effects of As combined with NPs and suggest that diet was the main driver for oysters exposure to NPs. Therefore, the combined NPs + As treatments triggered a

552 synergetic effect that most likely increased the number of mitochondria. The
553 expression of *gadd45* for NPG + As treatment at 100 µg L^{-1} was not significantly
554 different from its control nor the As alone treatment. Yet, it significantly decreased
555 compared to NPG at 100 µg L^{-1}. This indicates that the expression of *gadd45* for
556 NPG treatment at 100 µg L^{-1} was prevented in combination with As. The expression
557 of *p53* for NPG + As treatment at 100 µg L^{-1} did not significantly change compared to
558 the control and the As alone treatments, but its expression significantly increased
559 compared to NPG + As at 10 µg L^{-1} (**Fig. 6 D**). The expression of *p53* for PSL
560 treatment at 100 µg L^{-1} did not significantly change compared to the control, but its
561 expression significantly increased compared to the PSL + As at 100 µg L^{-1} and to
562 PSL at 10 µg L^{-1} treatments. Thereby, PSL treatment at 100 µg L^{-1} in combination
563 with As prevented *p53 gene* expression (**Fig. 6 E**). Overall, the exposure to As in
564 NPG + As treatment at 100 µg L^{-1} significantly changed *gadd45* and *p53* expressions
565 relatively to NPG treatment for the same concentration. The opposite *gadd45* and
566 *p53* responses to NPG + As treatment might be caused by several negative
567 feedback loops (Harris and Levine, 2005). Indeed *gadd45* regulation is (among
568 others) upon P53 transcription factor, hence its downregulation can be linked to P53
569 increase (Salvador *et al.*, 2013). The expression of *bcl-2* significantly increased in
570 the PSL treatment at 100 µg L^{-1} compared to control and to PSL at 10 µg L^{-1}
571 treatments (**Fig. 6 G**). The *bcl-2* expression for PSL at 100 µg L^{-1} also significantly
572 increased compared to As treatment, but not to PSL + As at 100 µg L^{-1}. Thereby, the
573 expression of *bcl-2* for PSL treatment at 100 µg L^{-1} was prevented in combination
574 with As. Despite being an anti-apoptotic gene (Aouacheria, 2005), *bcl-2* upregulation
575 has been associated with a significant decrease of red granulocyte percentage in
576 clams blood exposed to MPs (Tang *et al.*, 2019).

577

578 *3.4.2 Combined effects of arsenic with nanoplastics*

579 We observed specific gene responses for combined NPs + As treatments in both
580 tissues. A single antagonist effect was measured (**Fig. 5 A**), while consistent
581 synergetic effects were measured (**Fig. 5 B, 6 C**). Synergetic effects, according to
582 Bhagat *et al.* (2020) definition, were identified by genes upregulation for NPs + As
583 treatments significantly different from control, As and NP treatments alone. As such,

NPG + As and PSC + As synergetic effects on *12S* expression revealed an increase of rRNA level produced by mitochondria that could indicate the induction of mitochondria number in visceral mass (**Fig. 6 C**). Yet, presumed toxicity on mitochondrial metabolism (e.g., oxidative stress) cannot be associated with the results since antioxidant gene responses of *cat*, *sod,* and *gapdh* were not consistent. Interestingly, Freitas *et al.* (2018) measured a significant inhibition of electron transport system activity, with significant inductions of superoxide dismutase and catalase activities in clams exposed to combined multi-walled carbon nanotubes. Synergetic or antagonist effects have been observed for several combined contaminants (Kim *et al.*, 2017; Bhagat *et al.*, 2020) and are most likely related to contaminant changes in bioavailability and/or speciation (Spurgeon *et al.*, 2020). In our experiment *T. lutea* potentially biotransformed As, but only in NPs + As treatments. These As speciation changes might have been reduced by the presence of NPs. Indeed, *T. lutea* was very likely shortly exposed to As before being consumed by *C. virginica*. Thus, As have been potentially metabolized by *T. lutea* as documented for microalgae (Cullen and Reimer, 1989; Azizur Rahman *et al.*, 2012). For instance, phytoplankton and bacteria are major producers of As methylated forms (e.g., dimethylarsinous acid, monomethylarsonous acid; Wood, 1974; Francesconi and Edmonds, 1996; Hellweger and Lall, 2004). However, in the presence of NPs, adsorbed inorganic As is potentially not available for *T. lutea* methylation. According to Farrell *et al.* (2011), adsorption can affect As speciation. These observations matter for toxicity assessment using gene expression responses since As methylated and inorganic forms have distinct molecular targets, bioaccumulation rates and excretion pathways (Dixon, 1997; Petric *et al.*, 2001; Hughes, 2002; Ng, 2005). Thereby As methylated forms present in As treatment may triggered different mRNA level responses from inorganic As present in NPs + As treatment. In this study, putative quantities of As methylated forms in As treatment might be less effective since we observed no significant changes for any investigated gene. Inorganic As forms are known to be more toxic than As methylated forms (Sephar *et al.*, 1980; Neff, 1997; Petric *et al.*, 2001, Ng 2005). Therefore, comparatively to As treatment, higher amounts of inorganic As available for *C. virginica* could explain synergetic effects measured for NPs + As treatments.

We revealed herein synergetic effects in *C. virginica* exposure in contrast with the protective effects measured in *I. alatus* exposure, potentially driven by both species different physiology and sensitivity to As. These gene expression differences between both oyster species for As + NP treatments need to be considered in light of their respective As bioaccumulation. Therefore, the gene expression results from combined As + NP treatments highlighted the relevance of comparative species studies. As such the natural background and biology differences (observed for As bioaccumulation) led to contrasted effects between Canadian farmed oysters *C. virginica* and Caribbean wild oysters *I. alatus*.

4. Conclusion

There is a current lack of relevance in the literature of NPs ecotoxicity that we addressed by comparing the effects of three NP models with a gradient of environmental relevancy. In regards to *C. virginica* gene responses, the most effective NPs treatment combined with As was PSC, while PSL was the most effective NPs treatment conducted alone. Yet, with NPG, all three NPs in presence of As showed synergetic effects in both tissues of *C. virginica*. Our trophic exposure shed light on significant synergetic effects measured in mitochondrial metabolism and apoptosis related genes at low NP concentrations (10 and 100 µg L^{-1}). These are novel results regarding As combination with environmentally representative NPs (NPG). Overall, there were more significant gene responses to NP treatments in visceral mass than in gills. These results suggest that NPs were more available or effective by dietary route as we expected. Furthermore, our BAF results compared between two oyster species revealed higher As uptake for Canadian farmed oysters *C. virginica* than Caribbean wild oysters *I. alatus*. This comparative approach provided valuable data that revealed the effects variability of combined As + NP treaments between two oyster species. Therefore, future studies should target the As speciation to better assess the As forms being adsorbed to NPs and the putative role of microalgae. A longer exposure time at lower As concentration will also be relevant to confirm the gene expressions and bioaccumulation data measured in this study.

5. Acknowledgments

We acknowledge Bruno Grassl, Hind El Hadri and Stephanie Reynaud (IPREM) for providing the polystyrene nanoparticles; and Réjean Tremblay (UQAR) for providing microalgae solutions. The authors would like to thank Joy Gaubert (INRS) for help with the molecular assays and Jean-François Dutil (INRS) for help with arsenic analyses. The authors also appreciated the helpful comments from Patrice Couture and the unknown referees.

6. Funding source

This work was financially supported by the Agence Nationale de la Recherche (ANR) in the PEPSEA program (ANR-17-CE34-0008-05) to MB and JG, the Centre National de la Recherche (CNRS) in the EC2CO INIAME program to MB and JG, and the Canada Research Chair program (950-23223) to VSL.

7. References

Aguirre-Rubí, J.R., Luna-Acosta, A., Etxebarría, N., Soto, M., Espinoza, F., Ahrens, M.J., Marigómez, I. 2017. Chemical contamination assessment in mangrove-lined Caribbean coastal systems using the oyster *Crassostrea rhizophorae* as biomonitor species. *Environmental Science and Pollution Research*, 25(14), 13396–13415.

Akberali, H.B., Earnshaw, M.J. 1982. Studies of the effects of zinc on the respiration of mitochondria from different tissues in the bivalve mollusc *Mytilus edulis (L.). Comparative Biochemistry and Physiology Part C: Comparative Pharmacology*, 72(1), 149–152.

Ali, H., Khan, E. 2019. Trophic transfer, bioaccumulation, and biomagnification of non-essential hazardous heavy metals and metalloids in food chains/webs—Concepts and implications for wildlife and human health. *Human and Ecological Risk Assessment: An International Journal*, 25(6), 1353–1376.

Alimi, O.S., Farner Budarz, J., Hernandez, L.M., Tufenkji, N. 2018. Microplastics and Nanoplastics in Aquatic Environments: Aggregation, Deposition, and Enhanced Contaminant Transport. *Environmental Science & Technology*, 52(4), 1704–1724.

Al Kaddissi, S., Legeay, A., Elia, A.C., Gonzalez, P., Floriani, M., Cavalie, I., Massabuau, J.-C., Gilbin, R., Simon, O. 2012. Mitochondrial gene expression, antioxidant responses, and histopathology after cadmium exposure. *Environmental Toxicology,* 29(8), 893–907.

Andrady, A.L. 2017. The plastic in microplastics: a review. *Marine Pollution Bulletin*, 119, 12–22.

Aouacheria, A., Brunet, F., Gouy, M. 2005. Phylogenomics of Life-Or-Death Switches in Multicellular Animals: Bcl-2, BH3-Only, and BNip Families of Apoptotic Regulators. *Molecular Biology and Evolution*, 22(12), 2395–2416.

Arini, A., Daffe, G., Gonzalez, P., Feurtet-Mazel, A., Baudrimont, M. 2014. Detoxification and recovery capacities of *Corbicula fluminea* after an industrial metal contamination (Cd and Zn): A one-year depuration experiment. *Environmental Pollution*, 192, 74–82.

687 Arini, A., Gourves, P.-Y., Gonzalez, P., Baudrimont, M. 2015. Metal detoxification and gene
688 expression regulation after a Cd and Zn contamination: An experimental study on *Danio rerio.*
689 *Chemosphere*, 128, 125–133.

690 Arthur, C., Baker, J., Bamford, H. 2009. Proceedings of the International Research Workshop on
691 the Occurrence, Effects, and Fate of Microplastic Marine Debris, 2008. National Oceanic and
692 Atmospheric Administration*, Technical Memorandum NOS-OR&R-30.*

693 Ashton, K., Holmes, L., Turner, A. 2010. Association of metals with plastic production pellets in
694 the marine environment. *Marine Pollution Bulletin*, 60, 2050–2055.

695 Azizur Rahman, M., Hasegawa, H., Peter Lim, R. 2012. Bioaccumulation, biotransformation and
696 trophic transfer of arsenic in the aquatic food chain. *Environmental Research*, 116, 118–135.

697 Bank, M.S., Hansson, S.V. 2019. The Plastic Cycle: A Novel and Holistic Paradigm for the
698 Anthropocene. *Environmental Science & Technology*, 53(13), 7177–7179.

699 Barnes, D.K.A., Galgani, F., Thompson, R.C., Barlaz, M. 2009. Accumulation and fragmentation
700 of plastic debris in global environments. *Philosophical Transactions of the Royal Society B: Biological*
701 *Sciences*, 364(1526), 1985–1998.

702 Baudrimont, M., Arini, A., Guégan, C., Venel, Z., Gigault, J., Pedrono, B., Prunier, J., Maurice, L.,
703 Ter Halle, A., Feurtet-Mazel, A. 2019. Ecotoxicity of polyethylene nanoplastics from the North Atlantic
704 oceanic gyre on freshwater and marine organisms (microalgae and filter-feeding bivalves).
705 *Environmental Science and Pollution Research*, 27, 3746−3755.

706 Baun, A., Hartmann, N.B., Grieger, K., Kusk, K.O. 2008. Ecotoxicity of engineered nanoparticles
707 to aquatic invertebrates: a brief review and recommendations for future toxicity testing. *Ecotoxicology*,
708 17, 387−395.

709 Bendif, E.M., Probert, I., Schroeder, D.C., De Vargas, C. 2013. On the description of *Tisochrysis*
710 *lutea gen. nov. sp. nov.* and *Isochrysis nuda sp. nov.* in the Isochrysidales, and the transfer of
711 Dicrateria to the Prymnesiales (Haptophyta). *Journal of Applied Phycology*, 25, 1763−1776.

712 Bendif, E.M., Probert, I., Schroeder, D.C., De Vargas, C. 2014. Erratum to: On the description of
713 *Tisochrysis lutea gen. nov. sp. nov.* and *Isochrysis nuda sp. nov.* in the Isochrysidales, and the
714 transfer of Dicrateria to the Prymnesiales (Haptophyta). *Journal of Applied Phycology.*

715 Bergami, E., Pugnalini, S., Vannuccini, M.L., Manfra, L., Faleri, C., Savorelli, F., Dawson, K.A.,
716 Corsi, I. 2017. Long-term toxicity of surface-charged polystyrene nanoplastics to marine planktonic
717 species *Dunaliella tertiolecta* and *Artemia franciscana*. *Aquatic Toxicology*, 189, 159–169.

718 Besseling, E., Wang, B., Lurling, M., Koelmans, A.A. 2014. Nanoplastic Affects Growth of *S.*
719 *Obliquus* and Reproduction of *D. Magna*. *Environmental Science Technology*, 48, 12336−12343.

720 Bhagat, J., Nishimura, N., Shimada, Y. 2020. Toxicological interactions of
721 microplastics/nanoplastics and environmental contaminants: Current Knowledge and Future
722 Perspectives. *Journal of Hazardous Materials*, 123913.

723 Bouillon, S. 2011. Storage beneath mangroves. *Nature Geoscience*, 4(5), 282–283.

724 Bouwmeester, H., Hollman, P.C.H., Peters, R.J.B. 2015. Potential Health Impact of
725 Environmentally Released Micro- and Nanoplastics in the Human Food Production Chain:
726 Experiences from Nanotoxicology. *Environmental Science & Technology*, 49(15), 8932–8947.

727 Brennecke, D., Duarte, B., Paiva, F., Cacador, I., Canning-Clode, J. 2016. Microplastics as vector
728 for heavy metal contamination from the marine environment. *Estuarine Coastal and Shelf Science*,
729 178, 189–195.

730 Briand, N. 2014. Familles de plastiques et leurs usages. Septième continent. *MobiScience,*
731 *Briand.*

732 Browne, M.A., Galloway, T.S., Thompson, R.C. 2010. Spatial Patterns of Plastic Debris along
733 Estuarine Shorelines. *Environmental Science & Technology*, 44(9), 3404–3409.

Canesi, L., Ciacci, C., Fabbri, R., Balbi, T., Salis, A., Damonte, G., Cortese, K., Caratto, V., Monopoli, M.P., Dawson, K., Bergami, E., Corsi, I. 2016. Interactions of cationic polystyrene nanoparticles with marine bivalve hemocytes in a physiological environment: Role of soluble hemolymph proteins. *Environmental Research*, 150, 73–81.

Cao, R., Wang, D., Wei, Q., Wang, Q., Yang, D., Liu, H., Dong, Z., Zhang, X., Zhang, Q., Zhao, J. 2018. Integrative Biomarker Assessment of the Influence of Saxitoxin on Marine Bivalves: A Comparative Study of the Two Bivalve Species Oysters, *Crassostrea gigas*, and Scallops, *Chlamys farreri. Frontiers in Physiology*, 9.

Carpenter, E.J., Smith, K.L. 1972. Plastics on the Sargasso Sea surface. *Science*, 155, 1240−1241.

Carugati, L., Gatto, B., Rastelli, E., Lo Martire, M., Coral, C., Greco, S., Danovaro, R. 2018. Impact of mangrove forests degradation on biodiversity and ecosystem functioning. *Scientific Reports*, 8(1).

Chae, Y., An, Y.-J. 2017. Effects of Micro- and Nanoplastics on Aquatic Ecosystems: Current Research Trends and Perspectives. *Marine Pollution Bulletin*, 124, 624−632.

Cherkasov, A.S., Taylor, C., Sokolova, I.M. 2010. Seasonal variation in mitochondrial responses to cadmium and temperature in eastern oysters *Crassostrea virginica* (Gmelin) from different latitudes. *Aquatic Toxicology*, 97(1), 68–78.

Chiba, S., Saito, H., Fletcher, R., Yogi, T., Kayo, M., Miyagi, S., Ogido, M., Fujikura, K. 2018. Human footprint in the abyss: 30 year records of deep-sea plastic debris. *Marine Policy*, 96, 204–212.

Chipuk, J.E., Moldoveanu, T., Llambi, F., Parsons, M.J., Green, D.R. 2010. The BCL-2 Family Reunion. *Molecular Cell*, 37, 299–310.

Choi, K.-S., Lewis, D.H., Powell, E.N., Ray, S.M. 1993. Quantitative measurement of reproductive output in the American oyster, *Crassostrea virginica* (Gmelin), using an enzyme-linked immunosorbent assay (ELISA). *Aquaculture Research*, 24(3), 299–322.

Corsi, I., Cherr, G.N., Lenihan, H.S., Labille, J., Hassellov, M., Canesi, L., Dondero, F., Frenzilli, G., Hristozov, D., Puntes, V., Della Torre, C., Pinsino, A., Libralato, G., Marcomini, A., Sabbioni, E., Matranga, V. 2014. Common Strategies and Technologies for the Ecosafety Assessment and Design of Nanomaterials Entering the Marine Environment. *ACS Nano*, 8(10), 9694–9709.

Cullen, W.R., Reimer, K.J. 1989. Arsenic speciation in the environment. *Chemical Reviews*, 89, 713–764.

Davranche, M., Veclin, C., Pierson-Wickmann, A.-C., El Hadri, H., Grassl, B., Rowenczyk, L., Dia, A., Ter Halle, A., Blancho, F., Reynaud, S., Gigault, J. 2019. Are nanoplastics able to bind significant amount of metals? The lead example. *Environmental Pollution*, 249, 940–948.

Dawson, A.L., Kawaguchi, S., King, C.K., Townsend, K.A., King, R., Huston, W.M., Bengtson Nash, S.M. 2018. Turning microplastics into nanoplastics through digestive fragmentation by Antarctic krill. *Nature Communications*, 9(1).

Dixon, H.B.F. 1997. The biochemical action of arsonic acids especially as phosphate analogues. *Advanced Inorganic Chemistry*, 44, 191–227.

El Hadri, H., Gigault, J., Mounicou, S., Grassl, B., Reynaud, S. 2020a. Trace Element Distribution in Marine Microplastics Using Laser Ablation-ICP-MS. *Marine Pollution Bulletin*, 160, 111716.

El Hadri, H., Gigault, J., Maxit, B., Grassl, B., Reynaud, S. 2020b. Nanoplastic from mechanically degraded primary and secondary microplastics for environmental assessments. *NanoImpact*, 17.

Farrell, A.P., Brauner, C.J., Wood, C.M. 2011. Fish Physiology: Homeostasis and Toxicology of Essential Metals. *Elsevier Science*, 31 part B, 300–301.

Fortin, C., Campbell, P.G.C. 2000. Silver uptake by the green alga *Chlamydomonas reinhardtii in* relation to chemical speciation: Influence of chloride. *Environmental Toxicology and Chemistry*, 19(11), 2769–2778.

Francesconi, K.A., Edmonds, J.S. 1996. Arsenic and Marine Organisms. *Advances in Inorganic Chemistry*, 147–189.

Freitas, R., Coppola, F., De Marchi, L., Codella, V., Pretti, C., Chiellini, F., Morelli, A., Polese, G., Soares, A.M.V.M., Figueira, E. 2018. The influence of Arsenic on the toxicity of carbon nanoparticles in bivalves. *Journal of Hazardous Materials*, 358, 484–493.

Frias, J., Sobral, P., Ferreira, A.M. 2010. Organic pollutants in microplastics from two beaches of the Portuguese coast. *Marine Pollution Bulletin*, 60, 1988–1992.

Fronhoffs, S., Totzke, G., Stier, S., Wernert, N., Rothe, M., Brüning, T., Koch, B., Sachinidis, A., Vetter, H., Ko, Y. 2002. A method for the rapid construction of cRNA standard curves in quantitative real-time reverse transcription polymerase chain reaction. *Molecular and Cellular Probes*, 16, 99–110.

Galgani, F., Leaute, J., Moguedet, P., Souplet, A., Verin, Y., Carpentier, A., Goraguer, H., Latrouite, D., Andral, B., Cadiou, Y., Mahe, J.C., Poudlard, J.C., Nerisson, P. 2000. Litter on the Sea Floor Along European Coasts. *Marine Pollution Bulletin, 40(6), 516–527.*

Gall, S.C., Thompson, R.C. 2015. The impact of debris on marine life. *Marine Pollution Bulletin*, 92(1-2), 170–179.

Geißler, D., Gollwitzer, C., Sikora, A., Minelli, C., Krumrey, M., Resch-Genger, U. 2015. Effect of fluorescent staining on size measurements of polymeric nanoparticles using DLS and SAXS. *Analytical Methods*, 7(23), 9785–9790.

Gigault, J., Pedrono, B., Maxit, B., Ter Halle, A. 2016. Marine plastic litter: the unanalyzed nano-fraction. *Environmental Science: Nano*, 3(2), 346–350.

Gigault, J., Balaresque, M., Tabuteau, H. 2018a. Estuary-on-a-chip: unexpected results for nanoparticles fate and transport. *Environmental Science: Nano.*

Gigault, J., Ter Halle, A., Baudrimont, M., Pascal, P.-Y., Gauffre, F., Phi, T.-L., El Hadri, H., Grassl, B., Reynaud, S. 2018b. Current opinion: What is a nanoplastic? *Environmental Pollution*, 235, 1030–1034.

Gonzalez Araya, R., Mingant, C., Petton, B., Robert, R. 2012. Influence of diet assemblage on *Ostrea edulis* broodstock conditioning and subsequent larval development. *Aquaculture*, 364–365, 272–280.

Guillard, R.R.L. 1975. Culture of phytoplankton for feeding marine invertebrates. *Culture of Marine Invertebrate Animals*, 26–60.

Gutierrez-Galindo, E.A., Flores Muñoz, G., Villaescusa Celaya, J.A., Arreola Chimal, A. 1994. Spatial and temporal variations of arsenic and selenium in a biomonitor (*Modiolus capax*) from the Gulf of California, Mexico. *Marine Pollution Bulletin*, 28(5), 330–333.

Gutierrez-Villagomez, J.M., Martyniuk, C.J., Xing, L., Langlois, V.S., Pauli, B.D., Blais, J., Trudeau, V.L. 2019. Transcriptome Analysis Reveals that Naphthenic Acids Perturb Gene Networks Related to Metabolic Processes, Membrane Integrity, and Gut Function in *Silurana (Xenopus) tropicalis* Embryos. *Frontiers in Marine Science*, 6, 533.

Hancock, R. 2008. Recognising research on molluscs. *Australian Museum*. Archived from the original on 2009-05-03. Retrieved on 2009-03-09.

Harris, S., Levine, A. 2005. The p53 pathway: positive and negative feedback loops. *Oncogene*, 24, 2899–2908.

Hellweger, F.L., Lall, U. 2004. Modeling the Effect of Algal Dynamics on Arsenic Speciation in Lake Biwa. *Environmental Science & Technology*, 38(24), 6716–6723.

Holmes, L.A., Turner, A., Thompson, R. 2014. Interactions between trace metals and plastic production pellets under estuarine conditions. *Marine Chemistry*, 167, 25–32.

Hrenovic, J., Ivankovic, T. 2007. Toxicity of anionic and cationic surfactant to *Acinetobacter junii* in pure culture. *Open Life Sciences*, 2(3), 405–414.

Hughes, M. 2002. Arsenic toxicity and potential mechanisms of action. *Toxicology Letters*, 133, 1–16.

Jahan, K., Balzer, S., Mosto, P. 2008. Toxicity Of Nonionic Surfactants. *WIT Press*, 110, 281–290.

Johnson, A., Cronan, D.S. 2001. Hydrothermal Metalliferous Sediments and Waters Off the Lesser Antilles. *Marine Georesources & Geotechnology*, 19(2), 65–83.

Kim, D., Chae, Y., An, Y.J. 2017. Mixture toxicity of nickel and microplastics with different functional groups on *Daphnia magna*. *Environmental Science & Technology*, 51, 12852–12858.

Klinck, J.M., Powell, E.N., Hofmann, E.E., Wilson, E.A., Ray, S.M. 1992. Modeling oyster populations: the effect of density and food supply on production. *Proc. Adv. Mar. Tech. Conf.*, 5, 85–105.

Kobayashi, M., Hofmann, E.E., Powell, E.N., Klinck, J.M., Kusaka, K. 1997. A population dynamics model for the Japanese oyster, *Crassostrea gigas. Aquaculture*, 149(3-4), 285–321.

Koelmans, A.A., Besseling, E., Shim, W.J. 2015. Nanoplastics in the Aquatic Environment. Critical Review. *Marine Anthropogenic Litter*, 325–340.

Kraemer, L.D., Campbell, P.G.C., Hare, L. 2005. Dynamics of Cd, Cu and Zn accumulation in organs and sub-cellular fractions in field transplanted juvenile yellow perch (*Perca flavescens*). *Environmental Pollution*, 138(2), 324–337.

Kulkarni, R., Deobagkar, D., Zinjarde, S. 2018. Metals in mangrove ecosystems and associated biota: A global perspective. *Ecotoxicology and Environmental Safety*, 153, 215–228.

Lambert, S., Wagner, M. 2016. Characterisation of nanoplastics during the degradation of polystyrene. *Chemosphere*, 145, 265−268.

Langston, W.J. 1984. Availability of arsenic to estuarine and marine organisms: A field and laboratory evaluation. *Marine Biology*, 80, 143–154.

Lasareva, E.V., Parfenova, A.M., Demina, T.S., Romanova, N.D., Belyaev, N.A., Romankevich, E.A. 2017. Transport of the Colloid Matter of Riverine Runoff through Estuaries. *Oceanology*, 57(4), 520–529.

Lee, S.Y., Nam, Y.K. 2016. Evaluation of reference genes for RT-qPCR study in abalone Haliotis discus hannai during heavy metal overload stress. *Fisheries and Aquatic Sciences*, 19(1), 21.

Lenz, R., Enders, K., Nielsen, T.G. 2016. Microplastic exposure studies should be environmentally realistic. *Proceedings of the National Academy of Sciences*, 113(29), E4121–E4122.

Lucas, A., Beninger, P.G. 1985. The use of physiological condition indices in marine bivalve aquaculture. *Aquaculture*, 44(3), 187–200.

Luo, L., Ke, C., Guo, X., Shi, B., Huang, M. 2014. Metal accumulation and differentially expressed proteins in gill of oyster (*Crassostrea hongkongensis*) exposed to long-term heavy metal-contaminated estuary. *Fish & Shellfish Immunology*, 38(2), 318–329.

Lusher, A.L., McHugh, M., Thompson, R.C. 2013. Occurrence of microplastics in the gastrointestinal tract of pelagic and demersal fish from the English Channel. *Marine Pollution Bulletin*, 67(1-2), 94–99.

Lusher, A.L., Tirelli, V., O'Connor, I., Officer, R. 2015. Microplastics in Arctic polar waters: the first reported values of particles in surface and sub-surface samples. *Scientific Reports*, 5, 14947.

Lusher, A.L., Welden, N.A., Sobral, P., Cole, M. 2017. Sampling, isolating and identifying microplastics ingested by fish and invertebrates. *Analytical Methods*, *9*(9), 1346-1360.

Magrí, D., Sánchez-Moreno, P., Caputo, G., Gatto, F., Veronesi, M., Bardi, G., Catelani, T., Guarnieri, D., Athanassiou, A., Pompa, P.P., Fragouli, D. 2018. Laser Ablation as a Versatile Tool To Mimic Polyethylene Terephthalate Nanoplastic Pollutants: Characterization and Toxicology Assessment. *ACS Nano.*

Maher, W., Waring, J., Krikowa, F., Duncan, E., Foster, S. 2018. Ecological factors affecting the accumulation and speciation of arsenic in twelve Australian coastal bivalve molluscs. *Environmental Chemistry*, 15(2), 46.

Mao, Y., Li, H., Huangfu, X., Liu, Y., He, Q. 2020. Nanoplastics display strong stability in aqueous environments: Insights from aggregation behaviour and theoretical calculations. *Environmental Pollution*, 258, 113760.

Mattsson, K., Hansson, L.A., Cedervall, T. 2015. Nano-Plastics in the Aquatic Environment. *Environmental Science : Processes & Impacts*, 17, 1712−1721.

Mayer, L.M., Wells, M.L. 2012. Aggregation of Colloids in Estuaries. *Treatise on Estuarine and Coastal Science*, 4, 143–160.

McCarthy, M.P., Carroll, D.L., Ringwood, A.H. 2013. Tissue specific responses of oysters, *Crassostrea virginica*, to silver nanoparticles. *Aquatic Toxicology*, 138-139, 123–128.

Ministère de la Santé et du Mieux-être du Nouveau Brunswick, février 2005. Evaluation des risques à la santé humaine. Annexe A - Etude sur la santé dans la région de Belledun.

Mitra, A. 2013. Sensitivity of mangrove ecosystem to changing climate. *India: Springer*, 62, 43–157.

Moreira, A., Freitas, R., Figueira, E., Volpi Ghirardini, A., Soares, A.M.V.M., Radaelli, M., Guida, M., Libralato, G. 2018. Combined effects of arsenic, salinity and temperature on *Crassostrea gigas* embryotoxicity. *Ecotoxicology and Environmental Safety*, 147, 251–259.

Motulsky, H.J., Brown, R.E. 2006. *BMC Bioinformatics*, 7(1), 123.

Neff, J.M. 1997. Ecotoxicology of arsenic in the marine environment. *Environmental Toxicology and Chemistry*, 16(5), 917–927.

Nel, A., Xia, T., Madler, L., Li, N. 2006. Toxic Potential of Materials at the Nanolevel. *Science*, 311, 622−627.

Ng, J.C. 2005. Environmental Contamination of Arsenic and its Toxicological Impact on Humans. *Environmental Chemistry*, 2(3), 146.

Nguyen, B., Claveau-Mallet, D., Hernandez, L.M., Xu, E.G., Farner, J.M., Tufenkji, N. 2019. Separation and Analysis of Microplastics and Nanoplastics in Complex Environmental Samples. *Accounts of Chemical Research.*

Ozbay, G., Reckenbeil, B., Marenghi, F., Erbland, P. 2014. Eastern oyster (*Crassostrea virginica*) aquaculture and diversity of associated species.*Oysters: Biology, Consumption, and Ecological Importance.* NOVA Publishing. Book, 128.

Pan, K., Wang, W.-X. 2012. Reconstructing the Biokinetic Processes of Oysters to Counteract the Metal Challenges: Physiological Acclimation. *Environmental Science & Technology*, 46(19), 10765–10771.

Parsons, M.B., Cranston, R.E. 2005. Distribution, transport, and sources of metals in marine sediments near a coastal lead smelter in northern New Brunswick. Metals in the Environment Around Smelters at Rouyn-Noranda, Québec, and Belledune, New Brunswick: Results and Conclusions of the GSC-MITE Point Sources Project*. Bulletin*, 584.

Pessoni, L., Veclin, C., El Hadri, H., Cugnet, C., Davranche, M., Pierson-Wickmann, A.C., Gigault, J., Grassl, B., Reynaud, S. 2019. Soap- and metal-free polystyrene latex particles as a nanoplastic model. *Environmental Science: Nano*, 6, 2253–2258.

Petrick, J.S., Jagadish, B., Mash, E.A., and Aposhian, H.V. 2001. Monomethylarsonous acid (MMAIII) and arsenite: LD50 in hamsters and in vitro inhibition of pyruvate dehydrogenase. *Chemical Research in Toxicology*, 14, 651–656.

Pikuda, O., Xu, E.G., Berk, D., Tufenkji, N. 2018. Toxicity Assessments of Micro- and Nanoplastics Can Be Confounded by Preservatives in Commercial Formulations. *Environmental Science & Technology Letters*, 6(1), 21–25.

Quik, J.T.K., Vonk, J.A., Hansen, S.F., Baun, A., Van De Meent, D. 2011. How to assess exposure of aquatic organisms to manufactured nanoparticles? *Environment International*, 37(6), 1068–1077.

Richardson, S.D., Kimura, S.Y. 2020. Water Analysis: Emerging Contaminants and Current Issues. *Analytical Chemistry*, 92(1), 473–505.

Rochman, C.M., Hentschel, B.T., Teh, S.J. 2014. Long-term sorption of metals is similar among plastic types: Implications for plastic debris in aquatic environments. *PloS One*, 9, 85433.

Rodney, E., Herrera, P., Luxama, J., Boykin, M., Crawford, A., Carroll, M.A., Catapane, E.J. 2007. Bioaccumulation and tissue distribution of arsenic, cadmium, copper and zinc in *Crassostrea virginica* grown at two different depths in Jamaica Bay, New York. *In vivo*, 29(1), 16.

Rosety, M., Ordóñez, F.J., Rosety Rodríguez, M., Rosety, J.M., Rosety, I., Carrasco, C., Ribelles, A. 2001. Acute toxicity of anionic surfactants sodium dodecyl sulphate (SDS) and linear alkylbenzene sulphonate (LAS) on the fertilizing capability of gilthead (*Sparus aurata L.*) sperm. *Histology and Histopathology*, 16(3), 839–843.

Sadri, S.S., Thompson, R.C. 2014. On the quantity and composition of floating plastic debris entering and leaving the Tamar Estuary, Southwest England. *Marine Pollution Bulletin*, 81(1), 55–60.

Saed, K., Ismail, A., Omar, H., Kusnan, M. 2004. Heavy metal depuration in flat tree oysters *Isognomon alatus* under field and laboratory conditions. *Toxicological and Environmental Chemistry*, 86, 171–179.

Salvador, J.M., Brown-Clay, J.D., Fornace, A.J. 2013. Gadd45 in Stress Signaling, Cell Cycle Control, and Apoptosis. *Experimental Medicine and Biology*, 793, 1–19.

Santana, M.F.M., Moreira, F.T., Pereira, C.D.S., Abessa, D.M.S., Turra, A. 2018. Continuous Exposure to Microplastics Does Not Cause Physiological Effects in the Cultivated Mussel *Perna perna*. *Archives of Environmental Contamination and Toxicology*, 74, 594–604.

Schuler, M., Bossy-Wetzel, E., Goldstein, J.C., Fitzgerald, P., Green, D. R. 2000. p53 Induces Apoptosis by Caspase Activation through Mitochondrial Cytochrome c Release. *Journal of Biological Chemistry*, 275(10), 7337–7342.

Sirover, M.A. 2011. On the functional diversity of glyceraldehyde-3-phosphate dehydrogenase: Biochemical mechanisms and regulatory control. *Biochimica et Biophysica Acta - General Subjects*, 1810(8), 741–751.

Siung, M. 1980. Studies on the Biology of *Isognomon Alatus* Gmelin (Bivalvia: Isognomonidae) with Notes on Its Potential as a Commercial Species. *Bulletin of Marine Sciences*, 30(1), 90‑101.

Soegianto, A., Winarni, D., Handayani, U.S., Hartati. 2013. Bioaccumulation, Elimination, and Toxic Effect of Cadmium on Structure of Gills and Hepatopancreas of Freshwater Prawn *Macrobrachium sintangese* (De Man, 1898). *Water, Air, & Soil Pollution*, 224(5).

Sokolova, I.M., Sokolov, E.P., Ponnappa, K.M. 2005. Cadmium exposure affects mitochondrial bioenergetics and gene expression of key mitochondrial proteins in the eastern oyste*r Crassostrea virginica* Gmelin (Bivalvia: Ostreidae). *Aquatic Toxicology*, 73(3), 242–255.

Smith, D., Gaspar, T.R., Levi-Polyachenko, N., Kuthirummal, N., Sakar, S., Ringwood, A.H. 2020. The Bioreactivity and Sunlight Potentiation of Hybrid Polymer Nanoparticles in Oysters, *Crassostrea virginica. Environmental Science & Technology*, 54, 16, 10031–10038.

Spehar, R.L., Fiandt, J.T., Anderson, R.L., DeFoe, D.L. 1980. Comparative toxicity of arsenic compounds and their accumulation in invertebrates and fish. *Archives of Environmental Contamination and Toxicology*, 9(1), 53–63.

Spurgeon, D.J., Lahive, E., Schultz, C.L. 2020. Nanomaterial transformations in the environment: effects of changing exposure forms on bioaccumulation and toxicity. *Small*, 2000618.

969 Strady, E., Schäfer, J., Baudrimont, M., Blanc G. 2011. Tracing cadmium contamination kinetics
970 and pathways in oysters (*Crassostrea gigas*) by multiple stable Cd isotope spike experiments.
971 *Ecotoxicology and Environmental Safety*, 74(4), 600–606.

972 Sussarellu, R., Suquet, M., Thomas, Y., Lambert, C., Fabioux, C., Pernet, M.E.J., Le Goïc, N.,
973 Quillien, V., Mingant, C., Epelboin, Y., Corporeau, C., Guyomarch, J., Robbens, J., Paul-Pont, I.,
974 Soudan, P., Huvet, A. 2016. Oyster reproduction is affected by exposure to polystyrene microplastics.
975 *Proceedings of the National Academy of Sciences*, 113(9), 2430–2435.

976 Tang, Y., Rong, J., Guan, X., Zha, S., Shi, W., Han, Y., Du, X., Wu, F., Huang, W., Liu, G. 2019.
977 Immunotoxicity of microplastics and two persistent organic pollutants alone or in combination to a
978 bivalve species. *Environmental Pollution*, 258, 113845.

979 Ter Halle, A., Jeanneau, L., Martignac, M., Jardé, E., Pedrono, B., Brach, L., Gigault, J. 2017.
980 Nanoplastics in the North Atlantic Subtropical Gyre. *Environmental Science & Technology*, 5, 51(23),
981 13689–13697.

982 Thiagarajan, V., Iswarya, V., Seenivasan, R., Chandrasekaran, N., Mukherjee, A. 2019. Influence
983 of differently functionalized polystyrene microplastics on the toxic effects of P25 TiO2 NPs towards
984 marine algae *Chlorella sp*. *Aquatic Toxicology*, 207, 208–216.

985 Tien, C., Chen, C.S. 2013. Patterns of metal accumulation by natural river biofilms during their
986 growth and seasonal succession. *Archives of Environmental Contamination and Toxicology*, 64, 605–
987 616.

988 Tran, D., Ciret, P., Ciutat, A., Durrieu, G., Massabuau, J.C. 2003. Estimation of potential and
989 limits of bivalve closure response to detect contaminants: Application to cadmium. *Environmental*
990 *Toxicology and Chemistry*, 22(4), 914–920.

991 Tremblay, G.-H., Gobeil, C. 1990. Dissolved arsenic in the St Lawrence Estuary and the
992 Saguenay Fjord, Canada. *Marine Pollution Bulletin*, 21(10), 465–469.

993 Tristan, C., Shahani, N., Sedlak, T.W., Sawa, A. 2011. The diverse functions of GAPDH: Views
994 from different subcellular compartments. *Cellular Signalling*, 23(2), 317–323.

995 UNEP. 2001. Marine litter - trash that kills, *United Nations Environment Programme*.

996 Ünlü, M.Y., Fowler, S.W. 1979. Factors affecting the flux of arsenic through the mussel *Mytilus*
997 *galloprovincialis*. *Marine Biology*, 51, 209–219.

998 US Environmental Protection Agency. 2001. Chemical speciation of arsenic in water and tissue
999 by hydride generation quartz furnace atomic absorption spectrometry*. US EPA, Method 1632,*
1000 *Revision A, Office of Water, Washington, DC*. EPA-821-R-01-006.

1001 Vicient, C.M., Delseny, M. 1999. Isolation of Total RNA from *Arabidopsis thaliana* Seeds.
1002 *Analytical Biochemistry*, 268(2), 412–413.

1003 Wallner-Kersanach, M., Theede, H., Eversberg, U., Lobo, S. 2000. Accumulation and Elimination
1004 of Trace Metals in a Transplantation Experiment with *Crassostrea rhizophorae*. *Archives of*
1005 *Environmental Contamination and Toxicology*, 38(1), 40–45.

1006 Wang, S., Liu, M., Wang, J., Huang, J., Wang, J. 2020. Polystyrene nanoplastics cause growth
1007 inhibition, morphological damage and physiological disturbance in the marine microalga *Platymonas*
1008 *helgolandica. Marine Pollution Bulletin*, 158, 111403.

1009 Ward, J.E., Zhao, S., Holohan, B., Mladinich, K.M., Griffin, T.W., Wozniak, J., Shumway, S.E.
1010 2019. Selective ingestion and egestion of plastic particles by the blue mussel (*Mytilus edulis*) and
1011 eastern oyster (*Crassostrea virginica*): implications for using bivalves as bioindicators of microplastic
1012 pollution. *Environmental Science & Technology*, 53, 15, 8776–8784.

1013 Wilson, E.A., Powell, E.N., Wade, T.L., Taylor, R.J., Presley, B.J., Brooks, J.M. 1992. Spatial and
1014 temporal distributions of contaminant body burden and disease in Gulf of Mexico oyster populations:
1015 The role of local and large-scale climatic controls. *Helgoländer Merresunters.* 46:201–235.

1016 Winnebeck, E.C., Millar, C.D., Warman, G.R. 2010. Why Does Insect RNA Look Degraded?

Journal of Insect Science, 10(159), 1–7.

Wolle, M.M., Conklin, S.D. 2018. Speciation analysis of arsenic in seafood and seaweed: Part II—single laboratory validation of method. *Analytical and Bioanalytical Chemistry*, 410(22), 5689–5702.

Won, E.-J., Kim, K.-T., Choi, J.-Y., Kim, E.-S., Ra, K. 2016. Target organs of the Manila clam *Ruditapes philippinarum* for studying metal accumulation and biomarkers in pollution monitoring: laboratory and in-situ transplantation experiments. *Environmental Monitoring and Assessment*, 188(8).

Wood, J.M. 1974. Biological cycles for toxic elements in the environment. *Science*, *183*(4129), 1049–1052.

Wright, S.L., Kelly, F.J. 2017. Plastic and Human Health: A Micro Issue? *Environmental Science & Technology*, 51, 6634–6647.

Yanan, D. 2012. Integrated biomarker and molecular responses in marine bivalve following exposure to environmental contaminants: Implications for human and environmental health. Thesis of Plymouth University, United Kingdom.

Yang, H.C., Fu, H.L., Lin, Y.F., Rosen, B.P. 2012. Pathways of Arsenic Uptake and Efflux. *Current Topics in Membranes,* 69, 325–358.

Yap, C.K., Azmizan, A.R., Hanif, M.S. 2011. Biomonitoring of Trace Metals (Fe, Cu, and Ni) in the Mangrove Area of Peninsular Malaysia Using Different Soft Tissues of Flat Tree Oyster *Isognomon alatus. Water Air Soil Pollution*, 218, 19–36.

Zhang, W., Wang, W.-X., Zhang, L. 2013. Arsenic speciation and spatial and interspecies differences of metal concentrations in mollusks and crustaceans from a South China estuary. *Ecotoxicology*, 22(4), 671–682.

Zhang, W., Guo, Z., Zhou, Y., Liu, H., Zhang, L. 2015. Biotransformation and detoxification of inorganic arsenic in Bombay oyster *Saccostrea cucullata*. *Aquatic Toxicology*, 158, 33–40.

Zhang, Q., Qu, Q., Lu, T., Ke, M., Zhu, Y., Zhang, M., Zhang, Z., Du, B., Pan, X., Sun, L., Qian, H. 2018. The combined toxicity effect of nanoplastics and glyphosate on *Microcystis aeruginosa* growth. *Environmental Pollution*, 243, 1106–1112.

Zook, J.M., Rastogi, V., MacCuspie, R.I., Keene, A.M., Fagan, J. 2011. Measuring Agglomerate Size Distribution and Dependence of Localized Surface Plasmon Resonance Absorbance on Gold Nanoparticle Agglomerate Size Using Analytical Ultracentrifugation. *ACS Nano*, 5(10), 8070–8079.

Figures

Figure 1. Hydrodynamic diameters of NP particles measured by DLS using a Zetasizer nano zs. Size distribution for PSC dispersion with z-average of 692.4 ± 68.55 nm (A) and the corresponding number of nanoparticles (B). Size distribution for NPG dispersion with z-average of 1071 ± 30.65 nm (C) and the corresponding number of nanoparticles (D). Each NPG batch is presented with a different shade of grey.

Figure 2. Scanning Electron Microscopy (X8000) observation of carboxylated polystyrene nanospheres of latex (PSL) adsorbed on *T. lutea* exposed for 48 h to 0 µg L^{-1} (A), 10 µg L^{-1} (B), 100 µg L^{-1} (C), 1000 µg L^{-1} (D) and 5000 µg L^{-1} (E). Arrows indicate the presence of adsorbed PSL to microalgae. Of note, only 10 µg L^{-1} and 100 µg L^{-1} were used for the oyster diet exposure.

Figure 3. Arsenic bioaccumulation (µg/g, dry weight, mean + sd) in *C. virginica* gills and visceral mass (n = 4), after one week of exposure to 1 mg L^{-1} As and/ or 100 µg L^{-1} NPs.

Figure 4. Relative arsenic bioaccumulation (µg/g, dry weight, mean + sd) compared between *I. alatus* and *C. virginica* in gills and visceral mass (n = 4), after one week of exposure to 1 mg L^{-1} As. Asterisks show a significant difference ($p < 0.01$) assessed by Student's t test.

Figure 5. Relative gene expressions in *C. virginica* gills after one-week exposure to 1 mg L^{-1} As combined or not with 10 and 100 µg L^{-1} NPs. mRNA levels are presented for *12S* (A), *bax* (B), *gapdh* (C) and *mt* (D). All the values are presented as the mean + sd (n = 4-5) normalized by *ef1α* and *rpl7* genes. Different letters denote significant differences ($p < 0.05$) among treatments assessed by two-way ANOVA followed by Tukey post-hoc test. Bold, italic and capital letters are used for PSL, PSC and NPG treatments respectively.

Figure 6. Relative gene expressions in *C. virginica* visceral mass after one-week exposure to 1 mg L^{-1} As combined or not with 10 and 100 µg L^{-1} NPs. mRNA levels are presented for *cltc*, (A), *sod3* (B), *12S* (C), *gadd45* (D), *p53* (E), *bax* (F), *bcl-2* (G), *mdr* (H), and *vit* (I). All the values are presented as the mean + sd (n = 4-5) normalized by *ef1α* and *rpl7* genes. Different letters denote significant differences (*p*

1079 < *0.05*) among treatments assessed by two-way ANOVA followed by Tukey post-hoc
1080 test. Bold, italic and capital letters are used for PSL, PSC and NPG treatments
1081 respectively.

1082 **Supplementary file titles**

1083 **Supplementary file Figure S1 –** *C. virginica* biometric parameters.

1084 **Supplementary file Table S1 –** *C. virginica* targeted gene functions and optimized
1085 primer sets temperatures for qPCR.

1086 **Supplementary file Figure S2 –** *C. virginica* relative gene expressions in gills.

1087 **Supplementary file Figure S3 –** *C. virginica* relative gene expressions in visceral
1088 mass.

1089

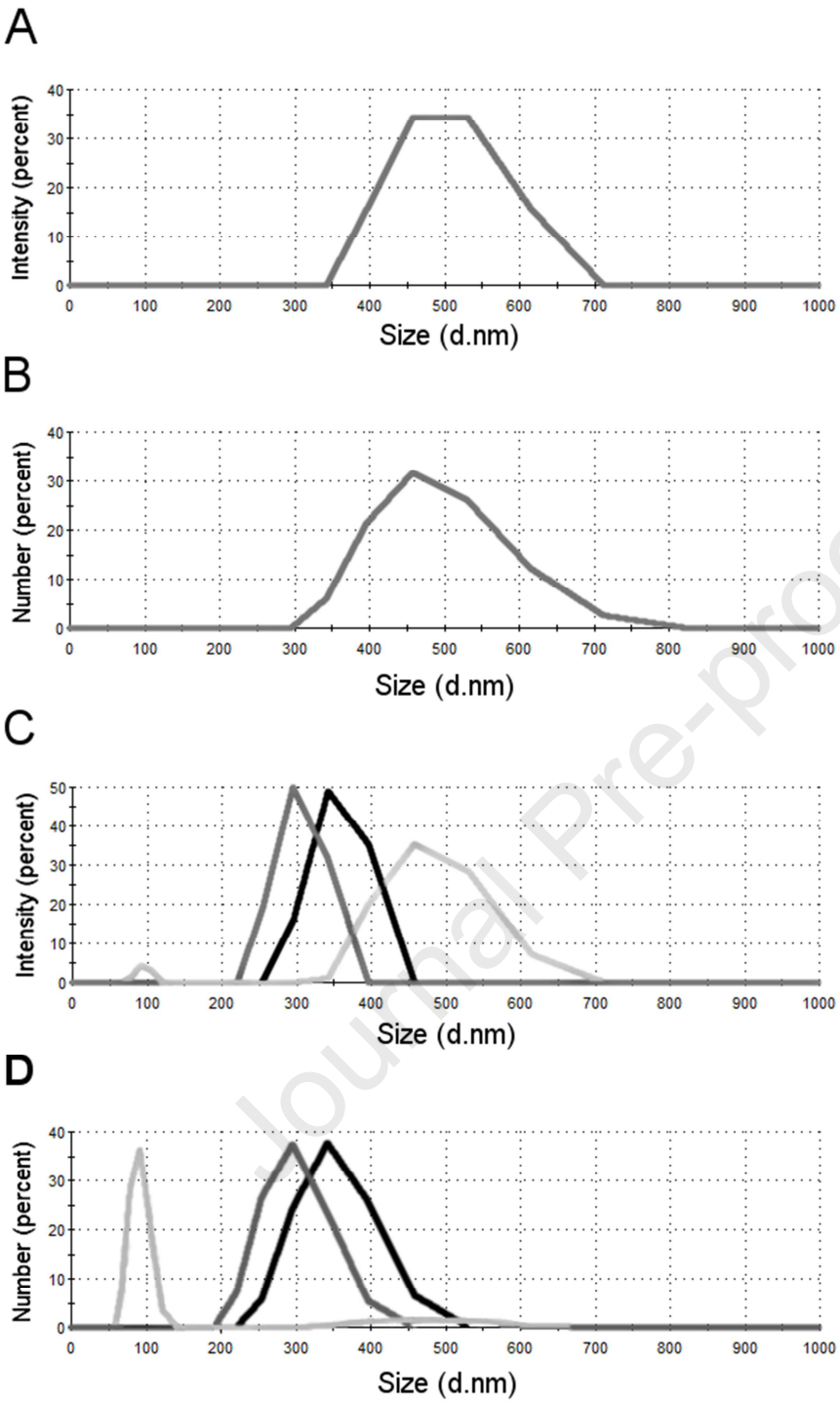

Figure 1. Hydrodynamic diameters of NP particles measured by DLS using a Zetasizer nano zs. Size distribution for PSC dispersion with z-average of 692.4 ± 68.55 nm (A) and the corresponding number of nanoparticles (B). Size distribution for NPG dispersion with z-average of 1071 ± 30.65 nm (C) and the corresponding number of nanoparticles (D). Each NPG batch is presented with a different shade of grey.

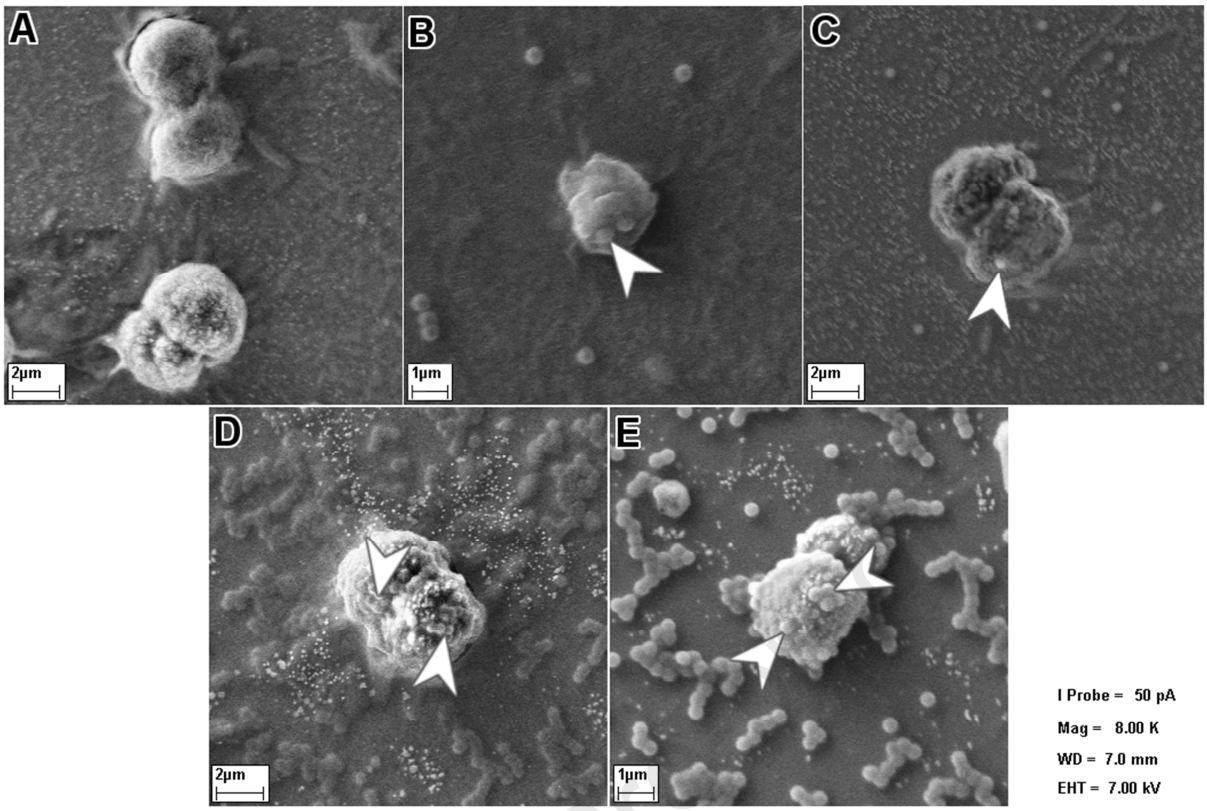

Figure 2. Scanning Electron Microscopy (X8000) observation of carboxylated polystyrene nanospheres of latex (PSL) adsorbed on *T. lutea* exposed for 48 h to 0, 10, 100, 1000, and 5000 µg L^{-1} (A - E). The arrows indicate the presence of adsorbed PSL to microalgae surface. Of note, only 10 µg L^{-1} and 100 µg L^{-1} were used for the oyster diet exposure.

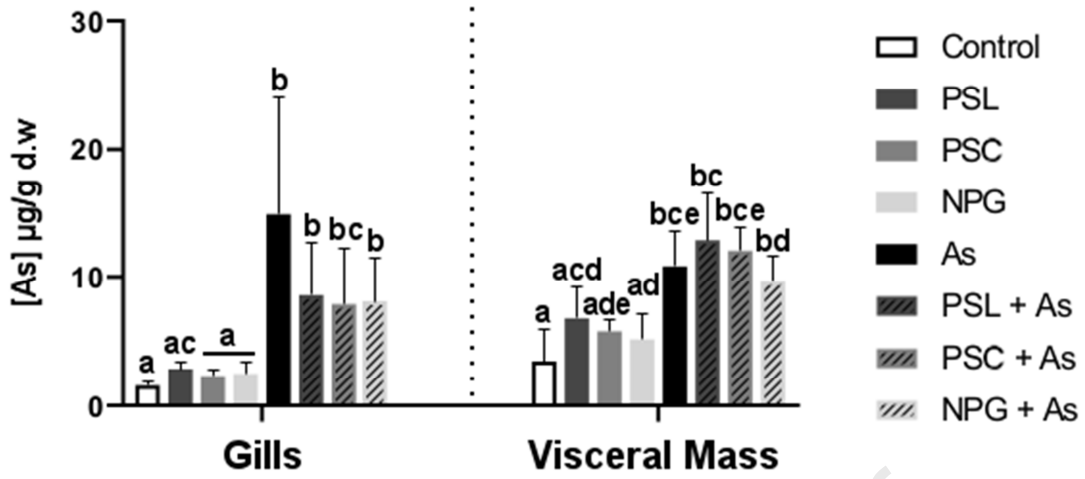

Figure 3. Arsenic bioaccumulation (µg/g, dry weight, mean + sd) in *C. virginica* gills and visceral mass, after one week of exposure to 1 mg L^{-1} As combined or not with 100 µg L^{-1} NPs. Different letters denote significant differences ($p < 0.05$) among treatments assessed by one-way ANOVA followed by Tukey post-hoc test (n = 4-5).

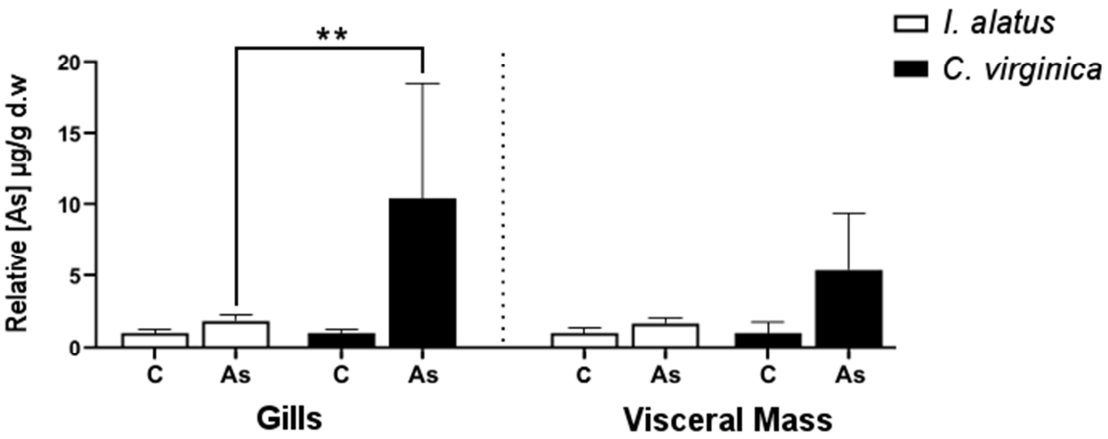

Figure 4. Relative arsenic bioaccumulation (µg/g, dry weight, mean + sd) compared between *I. alatus* and *C. virginica* in gills and visceral mass (n = 4), after one week of exposure to 1 mg L^{-1} As. Asterisks show a significant difference ($p < 0.01$) assessed by Student's t test.

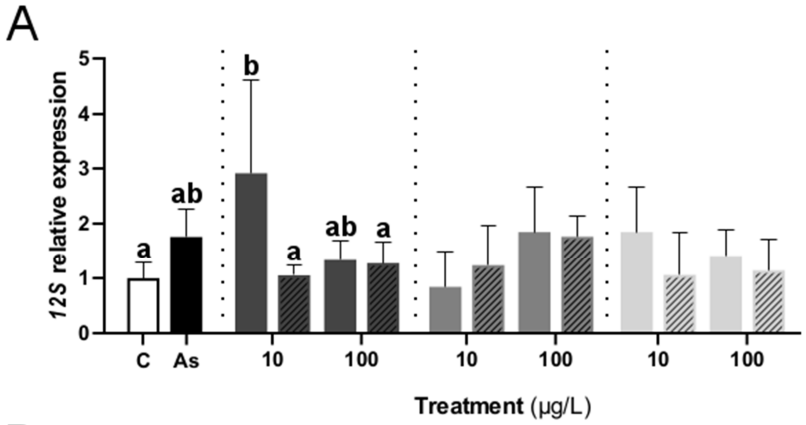

1121

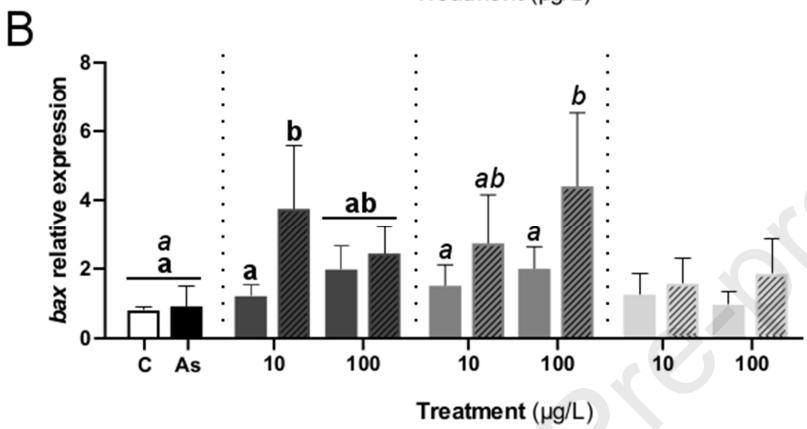

1122

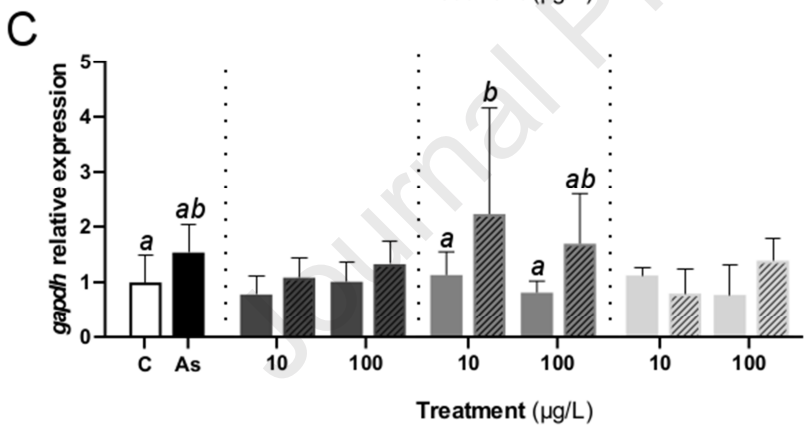

1123

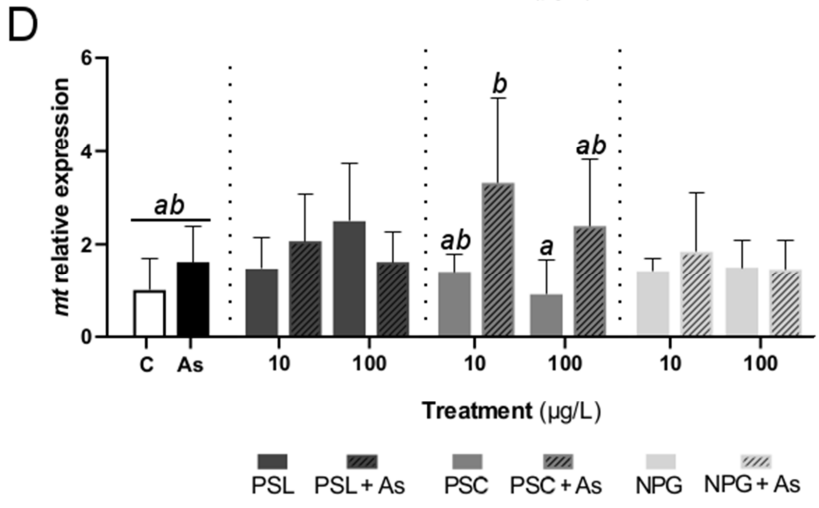

1124

Figure 5. Relative gene expressions in *C. virginica* gills after one-week exposure to 1 mg L^{-1} As combined or not with 10 and 100 µg L^{-1} NPs. mRNA levels are presented for *12S* (A), *bax* (B), *gapdh* (C) and *mt* (D). All the values are presented as the mean + sd (n = 4-5) normalized by *ef1α* and *rpl7* genes. Different letters denote significant differences ($p < 0.05$) among treatments assessed by two-way ANOVA followed by Tukey post-hoc test. Bold, italic and capital letters are used for PSL, PSC and NPG treatments respectively.

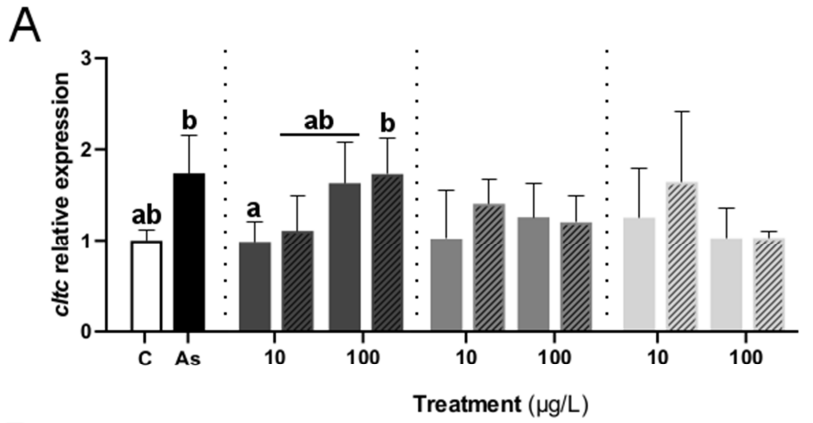

1133

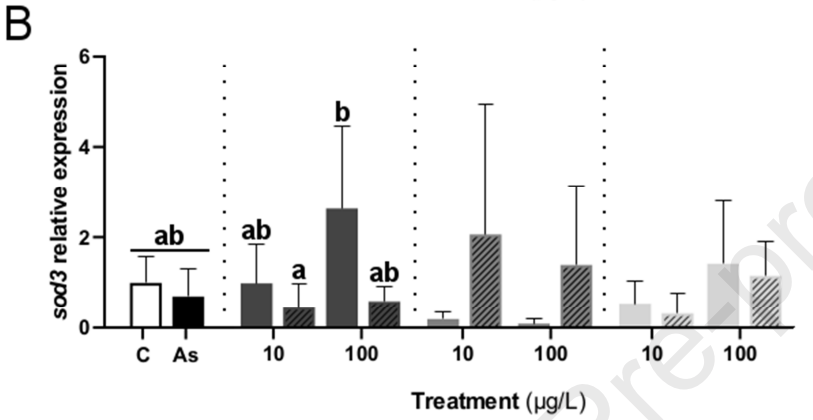

1134

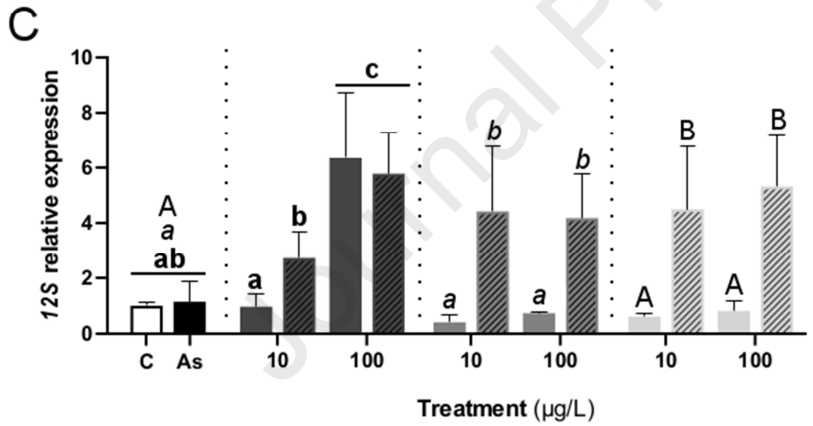

1135

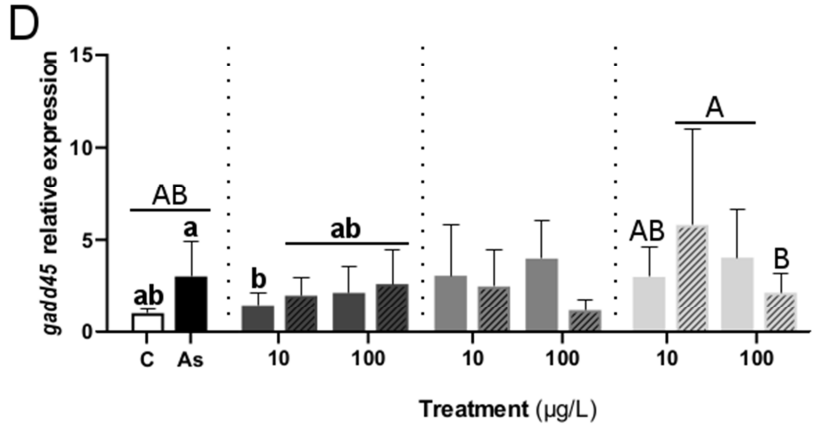

1136

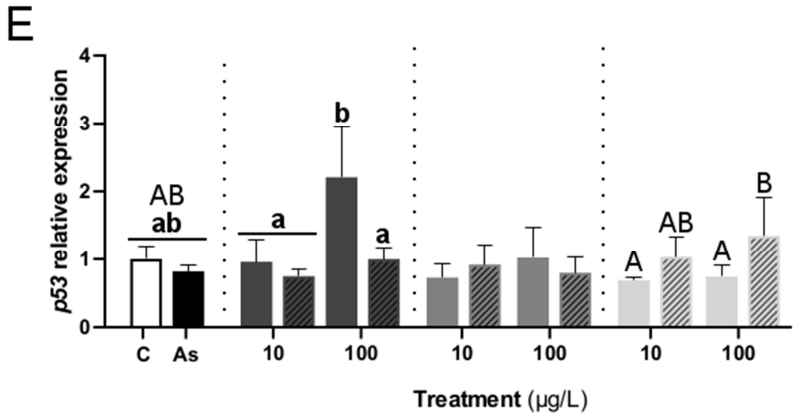

1137

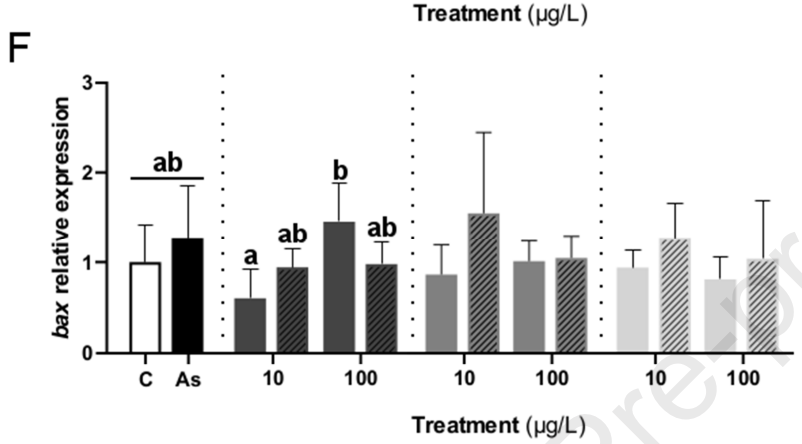

1138

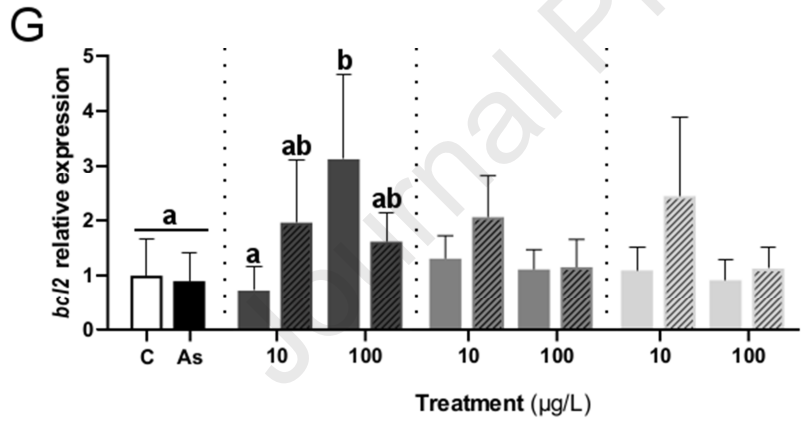

1139

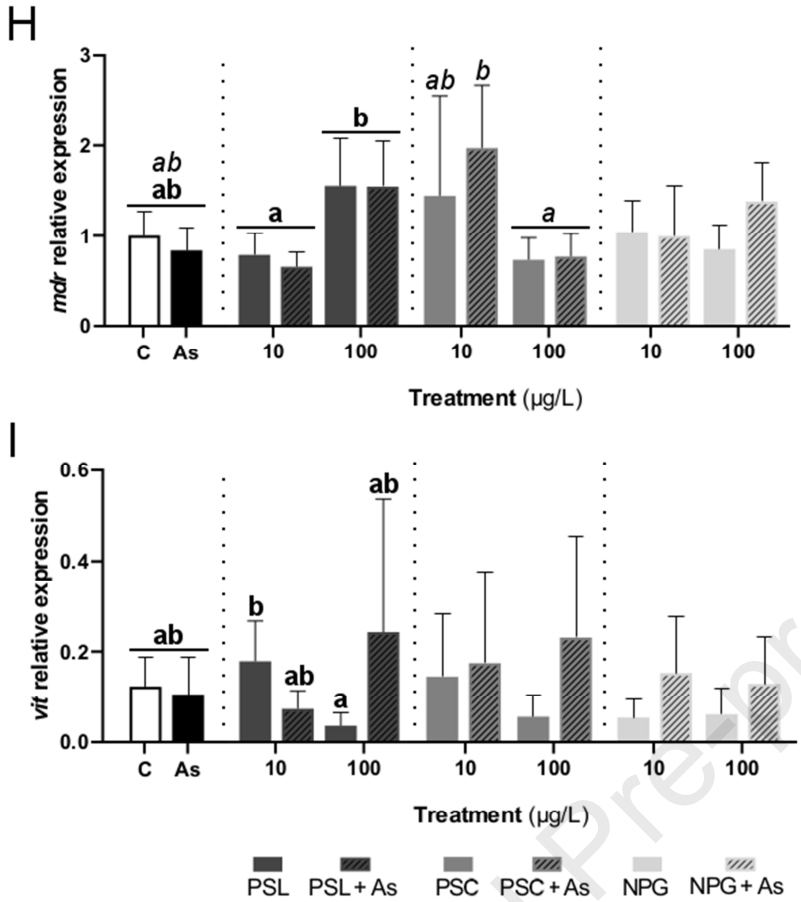

Figure 6. Relative gene expressions in *C. virginica* visceral mass after one-week exposure to 1 mg L^{-1} As combined or not with 10 and 100 µg L^{-1} NPs. mRNA levels are presented for *cltc*, (A), *sod3* (B), *12S* (C), *gadd45* (D), *p53* (E), *bax* (F), *bcl-2* (G), *mdr* (H), and *vit* (I). All the values are presented as the mean + sd (n = 4-5) normalized by *ef1α* and *rpl7* genes. Different letters denote significant differences ($p < 0.05$) among treatments assessed by two-way ANOVA followed by Tukey post-hoc test. Bold, italic and capital letters are used for PSL, PSC and NPG treatments respectively.

Highlights

- Nanoplastics are adsorbed on microalgae surface starting at 10 µg L^{-1} exposure.
- Nanoplastics triggered apoptotic and mitochondrial metabolism gene responses.
- The combination of nanoplastics with arsenic induced synergetic effects.
- Arsenic bioaccumulation did not increase in the presence of nanoplastics.

Declaration of interests

☒ The authors declare that they have no known competing financial interests or personal relationships that could have appeared to influence the work reported in this paper.

☐The authors declare the following financial interests/personal relationships which may be considered as potential competing interests: